Vol. 55: 169–187, 2009
doi: 10.3354/ame01287

AQUATIC MICROBIAL ECOLOGY
Aquat Microb Ecol

Printed May 2009
Published online April 23, 2009

Significance of diatom-derived polymers in carbon flow dynamics within estuarine biofilms determined through isotopic enrichment

B. J. Bellinger[1,4], G. J. C. Underwood[2], S. E. Ziegler[3], M. R. Gretz[1,*]

[1]**Department of Biological Sciences, Michigan Technological University, Houghton, Michigan 49931-1295, USA**
[2]**Department of Biological Sciences, University of Essex, Colchester, Essex CO4 3SQ, UK**
[3]**Department of Earth Sciences, Memorial University of Newfoundland, St. John's, Newfoundland A1B 3X5, Canada**

[4]***Present address:*** **Soil and Water Science Department, University of Florida, Gainesville, Florida 32611, USA**

ABSTRACT: Pennate diatoms are the main group of primary producers in transient microbial biofilms at the sediment surface in muddy intertidal systems. These microalgae produce a substantial quantity of extracellular polymeric substances (EPS) that contribute significantly to the cohesive properties observed in biofilms. Changes in carbohydrate content and composition and the persistence of diatom EPS were demonstrated with pulse-chase $NaH^{13}CO_3$ labeling and simultaneous detection of isotopic enrichment in polysaccharides and phospholipid fatty acids (PLFAs) in Colne Estuary, UK, biofilms over a 48 h period. Significant isotopic enrichment of glucan indicated that a large proportion of fixed carbon was initially sequestered into intracellular chrysolaminaran, and labeled carbon was also quickly used for production of the diatom PLFA 20:5ω3 and EPS. Saccharides in the EPS fractions were enriched rapidly, followed by labeling of distinct bacterial PLFAs through heterotrophic utilization of EPS within 4 h. Maximal isotopic enrichment of diatom and Gram-negative bacterial PLFAs and hot water- and hot bicarbonate-soluble EPS fractions occurred after 4 h, and ^{13}C-labeling increased in Gram-positive bacterial PLFAs throughout the study period. After 48 h, PLFAs remained highly labeled relative to diatom-derived polysaccharides, indicating persistence of assimilated C in organisms within the biofilms through time and rapid turnover of polysaccharide pools within the biofilms. Coupled pulse-chase isotopic labeling and simultaneous tracking of ^{13}C in polysaccharides and PLFAs directly demonstrated the flow of carbon between biofilm autotrophs and heterotrophic bacteria and the significance of diatom-derived carbohydrates in this exchange.

KEY WORDS: EPS · PLFA · Isotopic enrichment · Carbon pathways · Biofilms

INTRODUCTION

Biofilms at the surface of estuarine soft sediments represent a consortium of organisms, with pennate diatoms as the primary photoautotrophs (Underwood & Paterson 2003). The aggregation of motile diatoms and subsequent production of extracellular polymeric substances (EPS) at the sediment surface creates the cohesive film that promotes sediment stability (Underwood & Paterson 2003), and EPS content has been closely linked to algal primary productivity and biomass (Underwood & Smith 1998, Lucas et al. 2003). The significance of diatoms in EPS production has been shown by scanning electron microscopy (SEM) observations of surface biofilms (Paterson 1986) and by comparing polymer composition between diatom-dominated biofilms with unialgal diatom cultures (Bellinger et al. 2005). The biological polymers produced are carbohydrate-rich and consist of complex macromolecules that contribute significant biological advantages to the diatoms (Hoagland et al. 1993), other organisms within the biofilm matrix (Decho 2000, Underwood & Paterson

*Corresponding author. Email: mrgretz@mtu.edu

2003), and the environment in which these biofilms are found (e.g. through biostabilization; Paterson 1989, Lucas et al. 2003, Stal 2003). Recently, biofilm diatoms have been shown to respond to environmental changes by modifying their 'behavior' (movement modalities) with concomitant changes in chemical composition of EPS polysaccharides (Abdullahi et al. 2006, Apoya-Horton et al. 2006), highlighting the dynamic nature of EPS biopolymers and their role in biofilm ecology.

Rate of production and loss of diatom EPS vary over tidal cycles (Smith & Underwood 1998, de Brouwer & Stal 2001), and the polymers produced appear to be differentially susceptible to tidal wash-away and bacterial degradation (Hanlon et al. 2006). The effects of bacterial activity on polysaccharides within planktonic flocs have been well described, with bacteria showing fraction-specific preferences, i.e. high (HMW) versus low molecular weight (LMW), and monomer-specific preferences (Arnosti & Repeta 1994, Amon & Benner 1996, Giroldo et al. 2003). Significant relationships between bacterial production, chlorophyll *a* (chl *a*) and water-soluble (colloidal) carbohydrate content occur in estuarine benthic biofilms (van Duyl et al. 1999, 2000). Differences in bacterial growth efficiency and utilization of polysaccharides are attributed to compositional differences between fractions (Amon & Benner 1996). Compositional variability in LMW and HMW colloidal carbohydrates have been described for biofilms from the Colne Estuary, UK (Bellinger et al. 2005), and correlations between rates of bacterial enzymatic activity and degradation of complex HMW polymers were measured *in situ* by Hanlon et al. (2006). Increasing concentrations of either colloidal carbohydrate or ethanol-insoluble polymer (cEPS) content in sediment slurries resulted in enrichment of different bacterial communities, with *Gammaproteobacteria*, and especially *Acinetobacter*, stimulated by cEPS (Haynes et al. 2007). These data indicate that specific groups of bacteria may be adapted to use different components of the extracellular carbohydrates released by diatoms in biofilms.

Biomarkers are typically utilized to understand relationships between organisms and their environment on large scales. A distinctive group of biomarkers are phospholipid fatty acids (PLFAs), which are found in the membranes of most organisms (Vestal & White 1989, Volkman et al. 1989). PLFA profiles have been described for a number of bacterial groups (Vestal & White 1989, White et al. 1996), and are also diagnostic for algal groups (Volkman et al. 1989, Dunstan et al. 1994). In addition to distinguishing a variety of taxonomic groups, it is also possible to determine relative biomass based on the abundance of distinctive PLFAs, and more recently, determinations of $\delta^{13}C$ isotopic values have been coupled with PLFA identification, enabling food sources to be identified based on heterotrophic bacterial PLFA isotopic signatures (Abrajano et al. 1994, Boschker & Middelburg 2002, Veuger et al. 2006).

The use of natural carbon isotopic signatures is widespread in food web studies (Fry & Sherr 1984). However, ambiguity exists when interpreting natural isotope data, often due to a lack of significant separation in $\delta^{13}C$ of carbon sources, and consumption of a wide variety of resources by consumers, effectively 'mixing' the specific ratios of different types of carbon sources (Fry & Sherr 1984, Cloern et al. 2002). To overcome this, pulse ^{13}C-labeling has been employed for observing carbon flow through taxonomic groups in intertidal mudflats (Middelburg et al. 2000). The combined use of group-specific PLFAs and their isotopic signatures in complex communities has begun to shed light on the coupling between algae and bacteria and also of the flow of carbon within the bacterial loop (Middelburg et al. 2000). Recently, van Oevelen et al. (2006b) tracked carbon label through bacteria into invertebrates after ^{13}C-glucose labeling, and the retention of ^{13}C within bacterial peptidoglycans has been documented (Veuger et al. 2006, Cook et al. 2007). Middelburg et al. (2000) added seawater with ^{13}C-bicarbonate to biofilms, and subsequent $\delta^{13}C$-values observed in bacterial PLFAs were attributed to utilization of labeled colloidal carbohydrates produced by diatoms. They suggested that approximately 60% of photoassimilated carbon was rapidly excreted as EPS, values similar to those measured using ^{14}C labeling by Smith & Underwood (1998). Cook et al. (2007) measured a transfer of approximately 50% of microphytobenthos (MPB)-fixed carbon to bacteria within 24 h in experimental sandy-sediment mesocosms, but this transfer has not been directly measured in natural sediments. It is not well established to which extent different components of the EPS pool are utilized by bacteria, and which bacterial groups are the major heterotrophs using EPS. By tracking isotopic enrichment through individual monosaccharide residues of EPS polymers, pulse-chase ^{13}C-labeling experiments conducted on intact biofilm communities have the potential to determine which EPS components are utilized by bacteria. Experiments concerning the natural isotopic signatures of monosaccharides in organic matter have been carried out (Macko et al. 1990, 1998, van Dongen et al. 2001), including isotopic enrichment of monosaccharides in phytoplankton communities (Hama & Handa 1992, Goes et al. 1996), indicating the potential utility of this powerful tool for tracking carbon flow through diatom extracellular polysaccharides in estuarine biofilms.

The relationship between the production of algal-derived polysaccharides and utilization by bacteria with respect to carbon flow between photoautotrophs

and heterotrophic bacteria in intertidal mudflats remains to be directly shown (Boschker & Middelburg 2002). Recently, carbon budgets have been proposed for intertidal mudflats, concentrating on bacterial carbon and its fate (van Oevelen et al. 2006a,b, Veuger et al. 2006). However, since the work by Middelburg et al. (2000), there has been no ^{13}C-labeling work in natural muddy sediments focused on diatom EPS. In this investigation, we used a comprehensive qualitative approach to show the significant movement of carbon through well characterized diatom EPS fractions and demonstrate the role of diatom-derived polymer in carbon flow dynamics. Changes in carbohydrate content and composition over time are described relative to variations in algal biomass and grazing pressure. Pulse-chase labeling experiments with ^{13}C, coupled with carbon isotope measurements of diatom and bacterial-derived PLFAs and saccharide residues of diatom EPS, including analysis of intracellular and extracellular polysaccharide fractions, enabled tracking of carbon through these pools over multiple tidal cycles. In addition, isotopic analysis of characteristic diatom and bacterial PLFAs allowed determination of EPS uptake by specific bacterial groups and also demonstrated the intracellular flow of carbon within diatoms from storage polysaccharides to membrane lipids.

MATERIALS AND METHODS

Sampling. Experiments were carried out over a 48 h period, beginning on 26 May 2005, within a 4 × 4 m region of the intertidal, at mean tide level (MTL) at Alresford Creek (51° 50.2′ N, 0° 59.5′ E), Essex, UK. The MPB biofilms and water chemistry at this site in the Colne Estuary exhibit a well characterized (over a 15 to 20 yr period) pattern of species and nutrient concentrations (e.g. Kocum et al. 2002, Underwood et al. 2005, Hanlon et al. 2006, Thornton et al. 2007). Water column nitrate, silicate, and phosphate concentrations during late spring (May to June) are approximately 50, 25, and 6 µmol, respectively, with higher pore water concentrations (~200:50:9 µmol nitrate, silicate, phosphate, respectively). There is no evidence that the biofilms are nutrient-limited at this site, although short timescale micro-limitation within an actively photosynthesizing biofilm may occur.

During the morning mid-low tide, 144 PVC cores (internal diameter 6.5 cm, length 12 cm) were randomly placed, with the top of the core nearly flush with the sediment surface. Seawater collected the previous day during high tide was enriched with $NaH^{13}CO_3$ (Isotech, 98 atom % ^{13}C) to a final concentration of 0.2 g: 100 ml (Middelburg et al. 2000), and 50 ml were added to 72 designated cores. Non-labeled cores were placed slightly away from the ^{13}C-enriched cores to minimize cross contamination. Eighteen ^{13}C-enriched cores and 18 non-labeled (control) cores were collected (each core considered as an independent replicate) at 4 daylight, low-tide time points: 4, 12, 24, and 48 h after isotopic enrichment. Cores were returned to the laboratory within 20 min of collection for processing and sampling. The top 2 mm of sediment (active biofilm layer) were collected using syringes to extract the top layer for analysis of chl *a*, polysaccharides (Bellinger et al. 2005), and PLFAs (described below). Control PLFA biofilms from time point 4 h were lost prior to analysis. All biofilms (with the exception of those sampled for the motile community and invertebrates) were lyophilized and weighed prior to analysis and extraction. A sub-sample of biofilm material was acid treated to remove inorganic carbon prior to isotopic analysis. Briefly, ~10 mg of biofilm were acid fumed in a desiccator over concentrated HCl for 24 h; subsequently, a portion of each sample was directly treated with acid to verify that fuming was adequate to remove all inorganic carbon (Hedges & Stern 1984). Acid-treated samples were analyzed for %C and $\delta^{13}C$ on a Costech Elemental Analyzer 4010 interfaced to a $Delta_{plus}$ isotope ratio mass spectrometer (IRMS; Thermo-Finnigan) using a ConfloIII (Thermo-Finnigan) interface. Certified and internationally recognized isotopic standards were run at the beginning and end of each analysis. The precision of the certified isotopic standards was typically 0.2 to 0.5‰; thus, best analytical precision we report is ±0.25‰ for $\delta^{13}C$.

Motile algal community and invertebrates. To visualize the motile species assemblage in sediments, 3 intact control and enriched cores from each time point were covered with lens paper and exposed to light for 2 h, after which the lens paper was removed and rinsed into centrifuge tubes for microscopic analysis (Eaton & Moss 1966). The remaining 12 cm of sediment in the cores were sieved through 1 mm, 500 µm, and 300 µm sieves for invertebrate collection. Invertebrates (snails, polychaetes) were kept in 70% ethanol until they could be counted and identified, and densities are expressed as number m^{-2}.

Sediment chl *a* analysis. Three cores from control and enriched plots at each time point were analyzed for chl *a*. Four ml of 100% methanol (saturated with $MgCO_3$) were added to 100 mg of each biofilm sample, mixed, and incubated in the dark at 4°C for 24 h. Samples were mixed, then centrifuged (3000× *g*, 15 min) and the supernatant removed. Absorbance was measured at 665 and 750 nm (Hanlon et al. 2006). Samples were acidified and absorbance was again determined at the above wavelengths to correct for phaeopigment content. Chl *a* content was expressed as µg g^{-1} dry weight (dw) of biofilm.

Sediment polymer fractionation and colorimetric analysis. Three control and 3 enriched cores from each time point were sequentially extracted for algal-derived polymers as follows. Freeze-dried biofilm material was divided up for coarse (colorimetric) and fine (monosaccharide composition, isotopic signature) levels of analysis. Colloidal carbohydrates were extracted from ~100 mg of freeze-dried biofilm by addition of 4 ml of saline (25‰), vortex-mixing, and incubation for 30 min at 25°C. Following centrifugation (3000 × *g*, 15 min), 1 ml of supernatant was pipetted into boiling tubes, and total carbohydrate content was measured using the phenol-sulfuric acid assay as previously described (Underwood et al. 1995, Bellinger et al. 2005) with glucose as the standard. Carbohydrate content was expressed as µg g^{-1} dw biofilm and normalized to algal biomass as µg µg^{-1} chl *a*. One ml of supernatant was retained for total uronic acid content determination as previously described (Hanlon et al. 2006), using the Carbazole assay with galactuonic acid as the standard. Uronic acid content is reported as µg g^{-1} dw biofilm.

Following isolation of the easily-solubilized colloidal polymers, further sequential extraction was conducted using procedures developed for diatom cells and biofilms (Wustman et al. 1997, Bellinger et al. 2005). To defat and remove pigments from pellets remaining after colloidal extraction, 4 ml of ethanol were added, the mixture centrifuged (3000 × *g*, 15 min), and the supernatant discarded. Four ml of distilled water (dH_2O) were added to each pellet, mixed, and incubated at 95°C for 1 h. After centrifugation (3000 × *g*, 15 min), the supernatant (hot water-soluble [HW] fraction) was quantified for carbohydrates and uronic acids as above. A hot bicarbonate-soluble (HB) fraction was extracted from the pellet by addition of 4 ml of 0.5 mol l^{-1} $NaHCO_3$ and incubation at 95°C for 1 h. After centrifugation (3000× *g*, 15 min), the supernatant was removed and quantified for carbohydrates and for uronic acids as above. This sequential extraction procedure is effective in isolating loosely cell-associated, easily extracted colloidal carbohydrates (saline extract; Underwood et al. 1995, Hanlon et al. 2006), intracellular storage glucans (HW fraction; Wustman et al. 1997, Chiovitti et al. 2004, Abdullahi et al. 2006), and sheath/tightly cell-associated polymers (HB fraction; Wustman et al. 1997, Chiovitti et al. 2003a, Bellinger et al. 2005, Hanlon et al. 2006) from diatoms and biofilms.

PLFA isolation. Nine control and 9 enriched biofilm samples from each time point were subjected to lipid extraction. Lipids were extracted from ~5 g of freeze-dried material using a modified Bligh & Dyer method with a single phase extract of dichloromethane (DCM):methanol:0.05 M phosphate buffer (1:2:0.8) added to the biofilms and shaken in the dark for ~24 h (Findlay 2007). Lipids were separated into 3 classes, viz. neutral lipids, glycolipids, and phospholipids, on a silicic acid-H column, eluting with DCM, acetone, and methanol:water (10:1), respectively. All fractions were collected, dried, re-suspended in DCM and stored under N_2. Only the phospholipid fraction (methanol: water eluent) was analyzed further.

Polymer analysis. For monosaccharide analysis and carbon isotope determination of polymer fractions, freeze-dried biofilms (3 to 4 g from cores used in polymer fractionation) were sequentially extracted as described above using 6 volumes (approximately 30 ml) of solvent. All fractions were exhaustively dialyzed (6 to 8 kDa cut-off) overnight against dH_2O (water changed every 1 to 2 h) at 6°C and freeze-dried. Rinsing of sediments with ethanol and the dialysis were employed to de-salt (notably the sodium bicarbonate used for extraction) and to remove LMW materials and compounds (organic and inorganic) that may have been present.

Polymer isotopic signature analysis. For carbon isotope analysis of polymer fractions, 2.5 to 4 mg of freeze-dried extract were weighed into 5 × 9 mm tin capsules (Costech) and analyzed using a Costech Elemental Analyzer 4010 interfaced to a $Delta_{plus}$ IRMS (Thermo-Finnigan) using a ConfloIII (Thermo-Finnigan) interface. Mass of ^{13}C in a particular fraction was determined by multiplying atom % ^{13}C by the total carbon mass of a fraction.

Monosaccharide determination. Neutral monosaccharides were determined using methods described by Wustman et al. (1997). Briefly, 1 to 5 mg of freeze-dried carbohydrate extract were hydrolyzed in 2 M trifluoroacetic acid (TFA) at 121°C for 3 h, followed by reduction with $NaBH_4$ and acetylation with acetic anhydride to alditol acetates. Identification-quantitation was by gas chromatography-mass spectrometry (GC-MS; 20 m SP-2330 capillary column, 0.25 mm i.d., 70 cm^3 min^{-1}, 230°C isothermal) on a Magnum Ion Trap (Finnigan–MAT) and was based on mass spectra, relative retention times, and response factors relative to a standard sugar mixture with myo-inositol as the internal standard. Monosaccharides are reported as % of total detected (relative abundance, RA). Alditol acetates were stored dry at –20°C for later isotopic analysis (see below).

Monosaccharide isotopic analysis. Isotopic determination of monosaccharides (as alditol acetates) was carried out on an Agilent 6890 GC interfaced to a $Delta_{plus}$ IRMS via a GC-combustion (GC-C; Thermo Finnigan) interface. Samples were injected (split-less mode at 280°C) onto a 70% cyanopropyl polysilphenylene-siloxane (SGE BPX-70; 50 m length, 0.32 mm i.d., and 0.25 µm film thickness) column programmed from 90°C to 240°C at 50°C min^{-1}, held at 240°C for 25 min,

and then ramped to 280°C at 50°C min^{-1} with helium as the carrier gas. Analysis of an 8 sugar standard mixture (with inositol as the internal standard) allowed correction for the introduction of acetate carbon during acetylation, as well as the kinetic isotope effect associated with acetylation, which differs for each monosaccharide (Macko et al. 1998). The 8 sugar standard was subject to the same derivatization as unknown samples, and the isotopic composition of each alditol acetate was compared with its underivatized isotopic value determined by direct combustion-IRMS in order to calculate the correction factor required for each individual sugar (Silfer et al. 1991). Correction for acetylation of sugars ranged from 5 to approximately 20‰, similar to other studies (Teece & Fogel 2007). Analytical variation for replicate injections (n = 3) of unlabeled samples was <5‰. Replicate error in ^{13}C-labeled sugars was less than that observed for fatty acid methyl esters (FAMEs) (<20‰). The $\delta^{13}C$ of individual monosaccharides is expressed as per mil (‰) relative to Peedee Belemnite (PDB) corrected using known standards, and also as nmol excess ^{13}C g^{-1} dw biofilm for each saccharide. Excess ^{13}C (amount above background) was derived by calculating the atom % ^{13}C in enriched samples and subtracting the atom % ^{13}C in the control saccharides, giving the atom % excess (APE; Middelburg et al. 2000, Veuger et al. 2006). To calculate the atom % ^{13}C, the R value used for PDB was 0.01119490 (Flora et al. 2002). The APE was converted into nmol ^{13}C and normalized to g sediment extracted. Total ^{13}C present in neutral sugars was derived by multiplying the atom % for each sugar by the total carbon mass detected. The proportion of ^{13}C detected as neutral sugar given the total measured ^{13}C in a fraction was then determined.

PLFA analysis. The PLFA fraction was saponified and methylated based on the methods of Findlay (2007). Briefly, PLFAs were treated with 0.2 M KOH in methanol and heated at 37°C for 15 min. KOH was neutralized with the addition of 0.2 M acetic acid, and FAMEs were isolated by phase separation using hexane:ether (9:1, v:v) and water. FAMEs were cleaned on pre-conditioned C-18 columns using acetonitrile:ddH_2O (1:1, v: v) and eluted using 750 µl of hexane:DCM (95:5, v: v). Samples were dried under N_2, and 75 µl of internal standard ethyl ester (24:0) in hexane were added. A further 1 ml of hexane was added before analysis.

FAMEs were quantified by flame ionization detection (FID) on an Agilent 6890 GC with split-less injection at 280°C on a BPX-70 column (as above), and the temperature was programmed from 90°C and ramped to 150°C at 50°C min^{-1}, held for 5 min, ramped to 210°C at 1.5°C min^{-1}, ramped to 280°C at 30°C min^{-1}, and held for 10 min with helium as the carrier gas. FAMEs were identified using an Agilent 5973 mass selective detector interfaced to the same GC and using the GC column and parameters described above. Identification was based on retention time of known standards, including both individual FAMEs (Sigma Aldrich) and mixtures (bacterial FAME and 37 component FAME standards, Supelco), and comparison of mass spectra to a National Institute of Standards database.

FAME isotopic composition was analyzed using an Agilent 6890 GC interfaced to a $Delta_{plus}$ IRMS via a GC-C-III interface and using GC parameters described above for the GC-FID and GC-MS analyses. A standard mixture of 4 phospholipids (1,2-dimyristoyl-sn-glycero-3-phosphocholine; 1,2-diheptadecanoyl-sn-glycero-3-phosphocholine; 1,2-dinonadecanoyl-sn-glycero-3-phosphocholine; and 1,2-diheneicosanoyl-sn-glycero-3-phosphocholine), each with fatty acid moieties that were predetermined for carbon isotopic composition, was saponified and methylated with each set of 6 samples processed. The 4-phospholipid standard was analyzed by GC-C-IRMS prior to and following each set of 6 samples and was used to correct each fatty acid for the addition of the methyl carbon by mass balance from the known fatty acid $\delta^{13}C$ value of each phospholipid standard and the methylated value measured with each set (Silfer et al. 1991, Abrajano et al. 1994). This correction did not vary more than 0.5‰ among the 4 individual phospholipid standards within each standard mixture, and the average correction was <4‰ across all sets of samples analyzed. Analytical variation for replicate injections (n = 3) of unlabeled samples was <5‰. Analytical variation for replicated injections of FAMEs derived from the ^{13}C-labeled samples was greater and ranged from <1 to 300‰, as expected in highly enriched compounds, with the lowest variation in the less istopically labeled samples. PLFAs are expressed as $\delta^{13}C$ values, and also as nmol excess ^{13}C g^{-1} dw biofilm for each PLFA. Absolute content of ^{13}C for a particular PLFA and the total amount of ^{13}C in extracted PLFAs at a particular time point were determined by multiplying the measured PLFA C-content by the atom % ^{13}C for that lipid. The proportion of ^{13}C in the 2 biomolecule pools (neutral sugars and PLFAs) was compared to look at incorporation and absolute amount persisting through time. Excess ^{13}C was derived by calculating the atom % ^{13}C in each PLFA sample and subtracting an approximate atom % ^{13}C. Unlabeled values were not available for the sediment PLFAs in the present study due to the loss of samples from the 4 h time point and subsequent deposition of enriched biomass or organic matter into the control plots after tidal cover (12 h after enrichment). Baseline values of −20 and −30‰ were therefore used to provide a range in the estimated APE for the PLFA. These values are based on observations of ^{13}C natural abundance values for PLFAs isolated from

the Scheldt Estuary, located in northern Europe, reported by Boschker et al. (2005). The APE was converted into nmol ^{13}C and normalized to g dw biofilm extracted.

Statistical analysis. Cores were treated as independent replicates within each treatment area. Heterogeneity of measurements from biofilms was found to be minimal in previous research at this site when sampling on a similar scale (Hanlon et al. 2006), enabling cores to be treated as independent with minimal variability. A 2-way analysis of variance (ANOVA) was used on *Hydrobia ulvae* Pennant densities, polymer content, chl *a,* and chl *a*-normalized carbohydrate data for differences between treatment and time for ^{13}C-enriched and control samples. Significant differences between samples through time were determined when $F_{0.05,3,23} > 3.24$; for treatment effects when $F_{0.05,1,23} > 4.49$; and for interaction effects when $F_{0.05,3,23} > 3.24$ (Zar 1999). Regression analysis was performed on carbohydrate content data against chl *a* and also for uronic acid content against carbohydrate content. Statistical analyses were run on SPSS version 13.

RESULTS

Biofilm community dynamics

Microscopic observations of the algal community from lens tissue showed that diatoms were the dominant autotrophic component of the biofilms during the study period, with the most common genera being *Amphora*, *Cylindrotheca*, and *Navicula*. There were minimal cyanobacterial and green algal cells observed microscopically, consistent with previous community descriptions from Alresford Creek (Thornton et al. 2002, Underwood et al. 2005). Maximum algal biomass (as chl *a*) was observed in control samples after 12 h, declining thereafter; and in ^{13}C-enriched cores at 4 h and subsequently declining (Fig. 1A). In ^{13}C-enriched and non-enriched cores, significant changes in chl *a* content occurred over time ($p < 0.05$; Fig. 1), but these changes were not a result of the addition of ^{13}C-bicarbonate (i.e. there were no treatment effects, $p = 0.12$).

There was a significant increase in the density of the deposit-feeding gastropod *Hydrobia ulvae* in both the ^{13}C-enriched and control samples ($p < 0.05$; Fig. 1A). *H. ulvae* abundances reached a maximum in the labeled cores after 24 h, and after 48 h in the control samples. Although an apparent treatment effect on density was indicated ($p < 0.001$; Fig. 1A), this is likely due to the uneven migration of the populations of *H. ulvae* across the mudflat into the experimental area. Grazing resulted in a significant negative correlation between *H. ulvae* density and chl *a* content ($r = 0.73$, $p < 0.001$; Fig. 1B), indicating that *H. ulvae* had a significant impact on algal biomass during the study period.

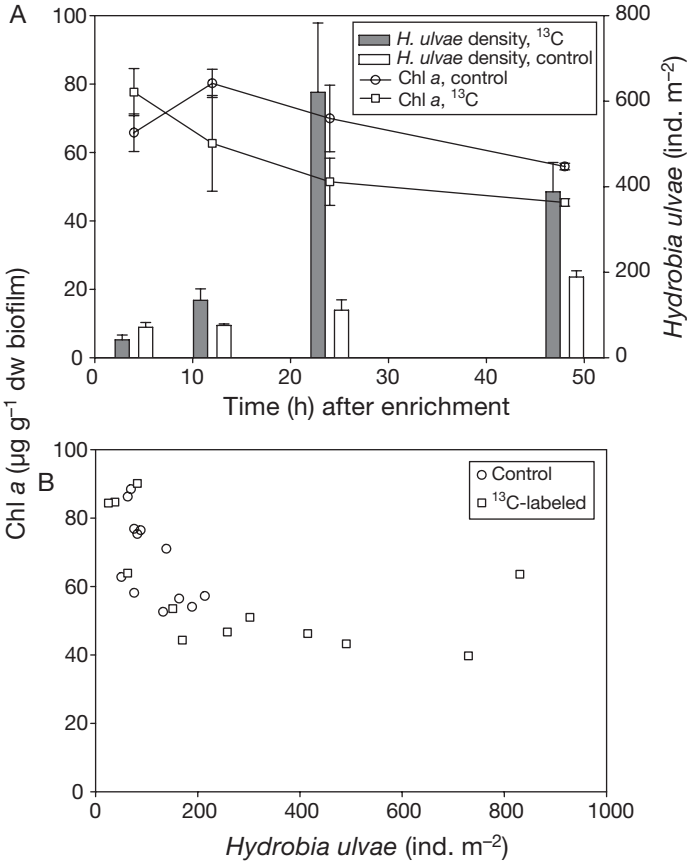

Fig. 1. (A) Algal biomass measured as chl *a* (left *y*-axis) and number of *Hydrobia ulvae* (right *y*-axis; means ± SEs; n = 3) isolated from Alresford Creek, UK. (B) Relationship between chl *a* and *H. ulvae* densities

Twenty-eight PLFAs were identified in our analysis in addition to 10 to 12 PLFAs of indeterminate unsaturation point(s). Total PLFA content measured ranged from 115 to 190 µg g^{-1} dw biofilm in the control cores and 147 to 268 µg g^{-1} in the ^{13}C-enriched cores. The most abundant PLFAs were 14:0, 16:0, 16:1ω7, 18:1ω7, and 20:5ω3. The former 2 are non-specific biomarkers, found in the membranes of many organisms (Findlay et al. 1990, Findlay 2007 and references therein). The PLFAs 18:1ω7 and 20:5ω3 are biomarkers for Gram-negative bacteria (Vestal & White 1989, Zelles 1997, Findlay 2007) and diatoms (Volkman et al. 1989, Dunstan et al. 1994), respectively. The PLFA 16:1ω7 has been found in abundance in cyanobacteria and Gram-negative bacteria, in addition to diatoms (Volkman et al. 1989). A number of Gram-positive bacterial biomarkers were identified, including i14:0, i15:0, and a15:0 (Vestal & White 1989, Findlay 2007 and references therein). Taken together, Gram-negative bacte-

ria had the largest contribution of between 10 and 20% of the total PLFA content, Gram-positive biomarkers represented approximately 9 to 12% of the total PLFA, and the sum of the diatom biomarkers 20:5ω3 and 16:2ω4 and 22:6ω3 represented between 5% and 10% of the total PLFA detected. A small amount of 18:2ω6 and 18:3ω3, indicative of cyanobacteria and green algae, was observed (each accounting for <1% of the total detected PLFA content) supporting the microscopic evidence for diatoms as the dominant autotrophic component in the biofilms studied.

Carbohydrate content

Within the control biofilms, maximum colloidal and HW carbohydrate content was observed at 12 h, coinciding with maximum algal biomass, and the carbohydrate content of these 2 fractions significantly declined thereafter ($p < 0.01$ and 0.005, respectively) (Fig. 2A). Within the ^{13}C-enriched samples, colloidal carbohydrates and HW carbohydrate content was at a maximum at 4 h and significantly declined by 48 h ($p < 0.05$ for both; Fig. 2A). There was no significant difference in HB carbohydrate content throughout the study period in treatment and control cores ($p = 0.969$ and 0.52, respectively; Fig. 2A). The 2-way ANOVA revealed significant treatment effects between control and ^{13}C-enriched samples for content of all 3 fractions (HW, colloidal, and HB, $p < 0.001$, 0.001, and 0.05, respectively).

There were significant correlations (pooling all time and treatment data) between chl *a* and colloidal carbohydrate content ($r = 0.52$, $p < 0.005$; Fig. 2B), and between HW carbohydrate content and chl *a* content ($r = 0.50$, $p < 0.05$; Fig. 2B). HB carbohydrate content did not show a correlation with chl *a* content ($r = 0.33$, $p = 0.115$; not shown), indicating that, unlike the colloidal and HW fractions, the HB fraction was not tightly correlated with autotrophic biomass in these biofilms.

Uronic acid content of fractions from treatment and control cores showed no consistent treatment effects or patterns of change with time. However, a significant correlation was observed between the carbohydrate content of a fraction and the uronic acid content ($r = 0.88$, $p < 0.001$; Fig. 2C), with uronic acid content approximately 20% of the total measured carbohydrate content of the different fractions extracted.

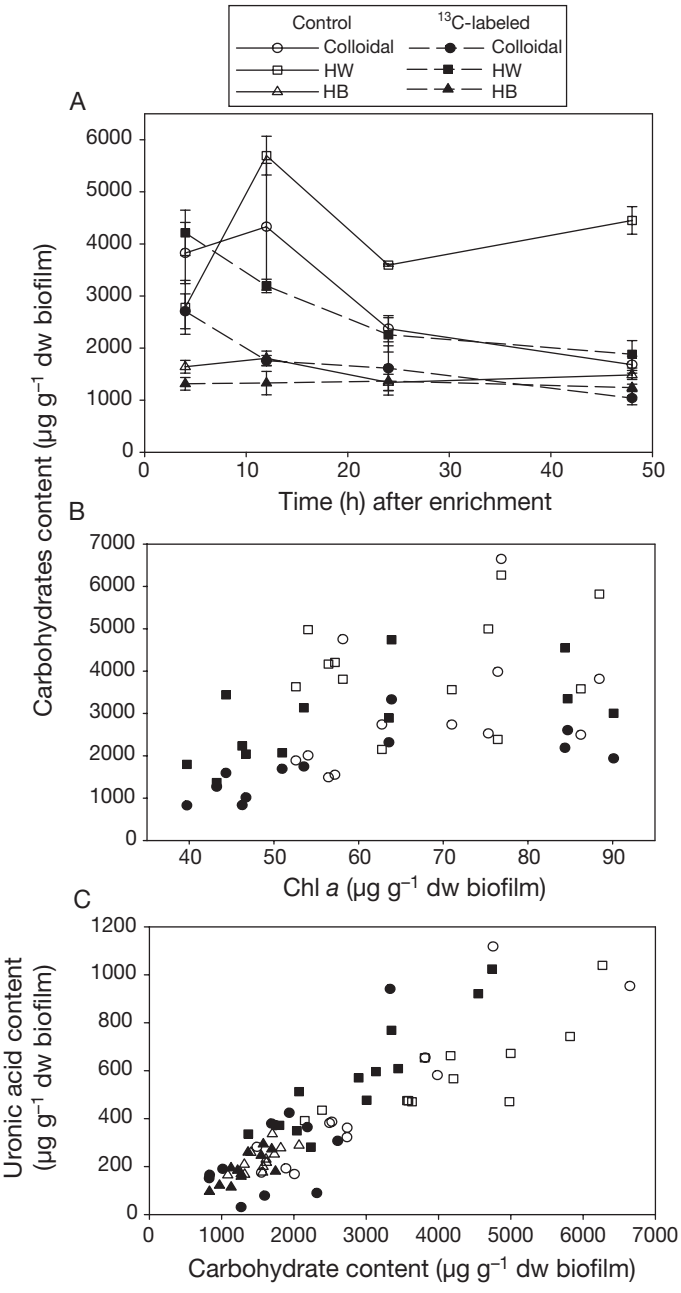

Fig. 2. (A) Carbohydrate content of fractions (colloidal; HW: hot-water soluble; HB: hot-bicarbonate soluble) isolated from biofilms (n = 3). (B) Relationship between algal biomass (as chl *a*) and colloidal carbohydrate content for all data from control and isotopically enriched plots. (C) Relationship between carbohydrate content and uronic acid content for all fractions

Monosaccharide analysis

Eight neutral sugars, viz. glucose (Glc), galactose (Gal), mannose (Man), xylose (Xyl), arabinose (Ara), ribose (Rib), fucose (Fuc), and rhamnose (Rha), were identified from hydrolyzates of sediment polymer fractions. Within each fraction, Glc showed the highest abundance relative to the other monosaccharides (Table 1). In the HW fraction of ^{13}C-labeled samples, Glc RA steadily declined over the sampling period, while in the control samples, Glc RA increased between the first 2 sampling periods but declined

Table 1. Relative abundance of monosaccharides in hydrolyzates of the colloidal, hot-water (HW) soluble, and hot-bicarbonate (HB) soluble fractions from control (c) and isotopically enriched (e) cores at Alresford Creek, UK. n = 3, with the exception of 48 h HW from the control. Means ± SD

Time (h) after enrichment	Treatment	Monosaccharides							
		Glucose (Glc)	Galactose (Gal)	Mannose (Man)	Xylose (Xyl)	Arabinose (Ara)	Ribose (Rib)	Fucose (Fuc)	Rhamnose (Rha)
Colloidal fraction									
4	e	51.4 ± 6.9	14.6 ± 2.3	8.0 ± 0.4	4.6 ± 1.6	2.2 ± 0.1	0.0	11.3 ± 0.9	7.9 ± 1.8
	c	25.0 ±6.4	16.3 ± 5.1	12.2 ± 0.5	5.7 ± 2.7	7.3 ± 6.9	0.5 ± 0.7	17.9 ± 1.1	15.1 ± 5.1
12	e	45.0 ± 14.6	16.1 ± 1.9	9.7 ± 1.6	4.9 ± 0.3	0.0	0.0	12.9 ± 5.1	11.4 ± 5.7
	c	39.8 ± 7.3	19.3 ± 3.5	11.9 ± 1.6	8.0 ± 1.9	2.2 ± 1.6	0.0	7.8 ± 1.9	11.1 ± 0.7
24	e	55.3 ± 0.7	14.5 ± 1.3	8.1 ± 1.5	4.7 ± 0.3	2.6 ± 1.0	0.0	8.7 ± 0.4	6.1 ± 0.8
	c	26.7 ± 1.6	25.9 ± 0.4	12.2 ± 2.7	10.3 ± 3.2	0.0	2.6 ± 3.7	11.1 ± 1.2	11.3 ± 0.1
48	e	44.4 ± 5.3	16.7 ± 1.4	9.8 ± 0.2	4.2 ± 0.6	3.4 ± 4.8	1.1 ± 1.5	11.8 ± 0.9	8.5 ± 0.3
	c	25.9 ± 4.3	20.1 ± 11.6	9.7 ± 0.3	6.2 ± 4.6	5.8 ± 1.1	1.8 ± 2.5	9.5 ± 4.6	21.1 ± 11.1
HW fraction									
4	e	70.9 ± 0.1	7.9 ± 1.2	6.1 ± 0.1	2.5 ± 0.9	1.5 ± 0.1	3.6 ± 0.8	3.5 ± 0.8	4.0 ± 0.5
	c	63.6 ± 5.5	9.0 ± 0.4	6.3 ± 0.5	2.9 ± 0.1	2.7 ± 0.9	5.8 ± 1.0	5.3 ± 1.7	4.3 ± 0.9
12	e	70.0 ± 0.4	13.1 ± 2.9	10.0 ± 2.4	2.4 ± 1.4	0.0	2.1 ± 2.9	0.0	2.5 ± 3.5
	c	87.8 ± 2.0	3.2 ± 0.8	2.7 ± 1.2	1.7 ± 0.2	0.0	1.8 ± 0.6	1.1 ± 0.1	1.7 ± 0.4
24	e	56.0 ± 8.9	11.9 ± 0.6	9.4 ± 0.1	3.6 ± 0.6	2.4 ± 3.4	6.6 ± 2.9	3.0 ± 1.2	7.2 ± 1.5
	c	69.7 ± 4.2	8.3 ± 1.6	5.8 ± 1.0	4.4 ± 0.4	0.0	4.6 ± 0.5	3.2 ± 0.3	4.1 ± 0.4
48	e	39.8 ± 4.0	17.7 ± 1.3	11.4 ± 0.7	4.3 ± 0.7	6.4 ± 3.4	3.2 ± 4.6	9.3 ± 2.7	7.9 ± 1.2
	c	63.1	5.7	6.1	7.2	2.0	3.9	5.8	6.2
HB fraction									
4	e	55.1 ± 15.4	15.6 ± 8.7	8.3 ± 3.1	4.5 ± 9.5	3.2 ± 1.3	2.6 ± 1.8	5.9 ± 5.6	4.8 ± 9.2
	c	55.0 ± 9.6	13.1 ± 0.9	7.9 ± 0.3	3.3 ± 0.5	3.0 ± 0.6	4.3 ± 0.9	7.9 ± 5.9	5.4 ± 0.5
12	e	61.4 ± 18.6	15.4 ± 1.7	7.9 ± 2.0	3.7 ± 2.1	2.7 ± 3.8	0.0	4.6 ± 6.6	4.2 ± 2.4
	c	71.3 ± 5.6	10.7 ± 2.3	6.2 ± 1.7	4.5 ± 0.3	0.0	0.0	3.3 ± 0.6	4.0 ± 0.7
24	e	62.0 ± 0.7	14.2 ± 2.7	9.3 ± 2.3	2.7 ± 1.0	4.6 ± 6.5	1.9 ± 2.7	0.0	5.4 ± 2.5
	c	58.0 ± 4.4	17.1 ± 3.1	9.5 ± 0.1	5.3 ± 0.7	0.0	0.9 ± 1.3	4.7 ± 1.1	4.4 ± 0.7
48	e	50.3 ± 6.3	14.8 ± 1.3	10.3 ± 1.4	3.1 ± 0.1	5.4 ± 3.8	3.2 ± 0.4	7.0 ± 1.7	5.8 ± 0.2
	c	32.7 ± 2.2	19.5 ± 3.5	6.0 ± 0.9	10.4 ± 4.6	10.3 ± 1.7	0.9 ± 1.3	9.3 ± 3.4	10.9 ± 0.5

thereafter (Table 1). Galactosyl and Man were the next most abundant saccharides in both labeled and non-labeled treatments, followed by Xyl, Fuc, and Rha (Table 1). Rib was present in the HW fraction, indicating extraction of RNA.

In the colloidal fraction, Glc RA was greater in ^{13}C-labeled cores (45 to 55%) than in control cores (25 to 40%; Table 1) and the RA of Gal, Man, and Xyl in the respective treatments changed very little over the course of the study, although comparison of treated and control samples revealed more variability. The proportions of the deoxy sugars Fuc and Rha in the colloidal fraction varied between ^{13}C-enriched and control samples, and also within treatment areas over time (Table 1).

The HB fraction was Glc-rich in control and ^{13}C-enriched samples (Table 1). Variation in the RA of Glc within each treatment followed trends similar to those observed in the HW fraction. A portion of this Glc in the HB fraction represents carry-over of chrysolaminaran due to incomplete extraction of the intracellular glucan during the hot water treatments (Abdullahi et al. 2006). The RA of the monosaccharides Gal, Man, and Xyl residues was similar between the colloidal and HB fractions. Galactosyl and Man were the most abundant saccharide residues after Glc in the HB fraction, with the deoxy sugars Fuc and Rha present throughout the study period (Table 1). Xyl and Ara content was highly variable between the beginning and end of the experiment in each treatment (Table 1).

Isotopic analysis — polymer fractions

Natural ^{13}C abundance values for intertidal mudflat polysaccharide fractions have not been previously reported. Colloidal carbohydrate fractions had δ^{13}C values of –16 to –11‰, HW fractions ranged from –15 to –10‰, and HB δ^{13}C-values varied between –17 and –13‰ (data not shown). Polysaccharide fractions showed intense isotopic labeling, the HW fraction at 4 h showed the largest initial labeling (Fig. 3), and enrichment of colloidal and HB soluble fractions followed similar trends (Fig. 3). The absolute amount of ^{13}C incorporated into the bulk fractions over the study period ranged from 0.5 µmol ^{13}C g^{-1} dw biofilm to 14 µmol ^{13}C g^{-1} dw biofilm. All fractions showed a large decline in ^{13}C content between 4 h and 12 h,

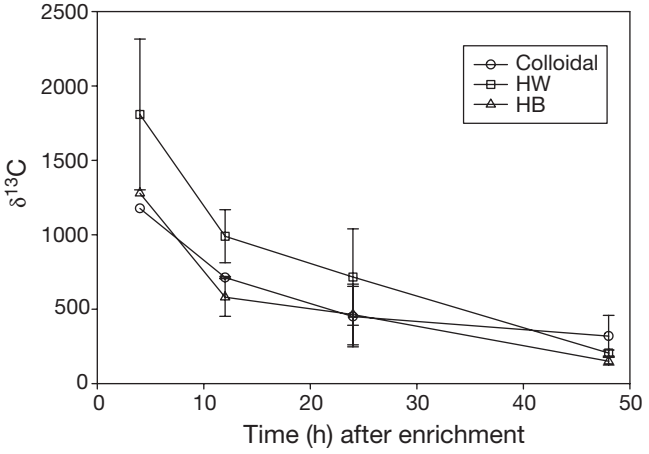

Fig. 3. $\delta^{13}C$ values of the total polymer fractions (colloidal; HW: hot-water soluble; HB: hot-bicarbonate soluble) from the isotopically enriched plot (means ± SE, n = 3)

and after 48 h, colloidal, HW, and HB fractions had similar isotopic signatures (Fig. 3), with the content of ^{13}C in the HB and colloidal fractions declining by half and the amount of ^{13}C in the HW fraction declining by 75%.

Isotopic analysis — EPS monosaccharides

With proper corrections for the addition of the acetate groups during the monosaccharide derivatization (Macko et al. 1998, Teece & Fogel 2007), all monosaccharides from control sample hydrolyzates were found to have $\delta^{13}C$-values between −2 and −18‰ (Table 2). Glc was one of the most $\delta^{13}C$-enriched sugars measured in control cores, a phenomenon observed in sugars produced by primary producers in culture conditions (Teece & Fogel 2007), which is indicative of rapid growth.

In the ^{13}C-treated samples, $\delta^{13}C$-values and enrichment patterns were not uniform across the range of glycosyl residues released from polymer fractions (Table 2). Within the HW fraction, Glc had the greatest enrichment after 4 h, and thereafter, excess ^{13}C declined steeply over the 48 h period (Fig. 4A, Table 2). A number of HW fraction saccharide residues had maximal excess ^{13}C after 24 h (Table 2, Fig. 4A), and enrichment patterns were unique to each saccharide (Fig. 4A). Excess ^{13}C in the hexosyl residues Gal and Man increased between 4 and 12 h and declined thereafter, while excess ^{13}C retained in the pentose Xyl and the deoxy-sugars Fuc and Rha decreased between 4 and 12 h and in-

Table 2. $\delta^{13}C$ (‰) isotopic ratios for monosaccharides from the enriched (e) and control (c) cores at Alresford Creek, UK (n = 1 for monosaccharides). n.d.: not determined; HW: hot-water soluble; HB: hot-bicarbonate soluble

Time (h) after enrichment	Treatment	Monosaccharides							
		Glucose (Glc)	Galactose (Gal)	Mannose (Man)	Xylose (Xyl)	Arabinose (Ara)	Ribose (Rib)	Fucose (Fuc)	Rhamnose (Rha)
Colloidal fraction									
4	e	302.6	84.4	46.9	26.2	12.7	0.0	65.9	45.3
	c	n.d.	n.d.	n.d.	n.d.	n.d.	n.d.	n.d.	n.d.
12	e	195.4	68.4	41.2	20.9	0.0	0.0	54.3	47.9
	c	−7.5	−13.8	−17.3	−8.6	−15.2	n.d.	−3.7	−18.2
24	e	296.9	77.7	43.6	25.4	13.7	0.0	46.6	32.9
	c	n.d.	n.d.	n.d.	n.d.	n.d.	n.d.	n.d.	n.d.
48	e	188.3	70.5	41.5	18.0	13.4	4.3	49.5	35.9
	c	n.d.	n.d.	n.d.	n.d.	n.d.	n.d.	n.d.	n.d.
HW fraction									
4	e	2972.8	336.6	255.5	110.4	64.6	148.0	140.8	166.6
	c	−2.0	−11.4	−15.7	−12.4	−16.8	−29.2	−4.5	−17.9
12	e	1673.2	286.2	215.9	43.8	0.0	77.0	0.0	90.8
	c	n.d.	n.d.	n.d.	n.d.	n.d.	n.d.	n.d.	n.d.
24	e	1705.8	356.6	280.0	104.0	58.0	185.1	86.0	209.7
	c	n.d.	n.d.	n.d.	n.d.	n.d.	n.d.	n.d.	n.d.
48	e	625.8	278.3	178.2	67.0	100.0	52.2	146.0	123.1
	c	n.d.	n.d.	n.d.	n.d.	n.d.	n.d.	n.d.	n.d.
HB fraction									
4	e	715.5	116.4	214.9	271.1	33.1	11.7	220.2	269.6
	c	−3.6	−13.9	−16.8	−13.9	−10.9	n.d.	−5.3	−18.5
12	e	614.5	157.9	82.1	38.8	29.9	0.0	93.8	44.5
	c	n.d.	n.d.	n.d.	n.d.	n.d.	n.d.	n.d.	n.d.
24	e	586.2	132.5	85.9	24.9	48.4	19.7	21.3	49.3
	c	−9.8	−14.2	−18.0	−12.4	−10.9	n.d.	−4.1	−19.2
48	e	517.5	152.1	103.3	31.9	51.2	32.1	69.1	58.8
	c	n.d.	n.d.	n.d.	n.d.	n.d.	n.d.	n.d.	n.d.

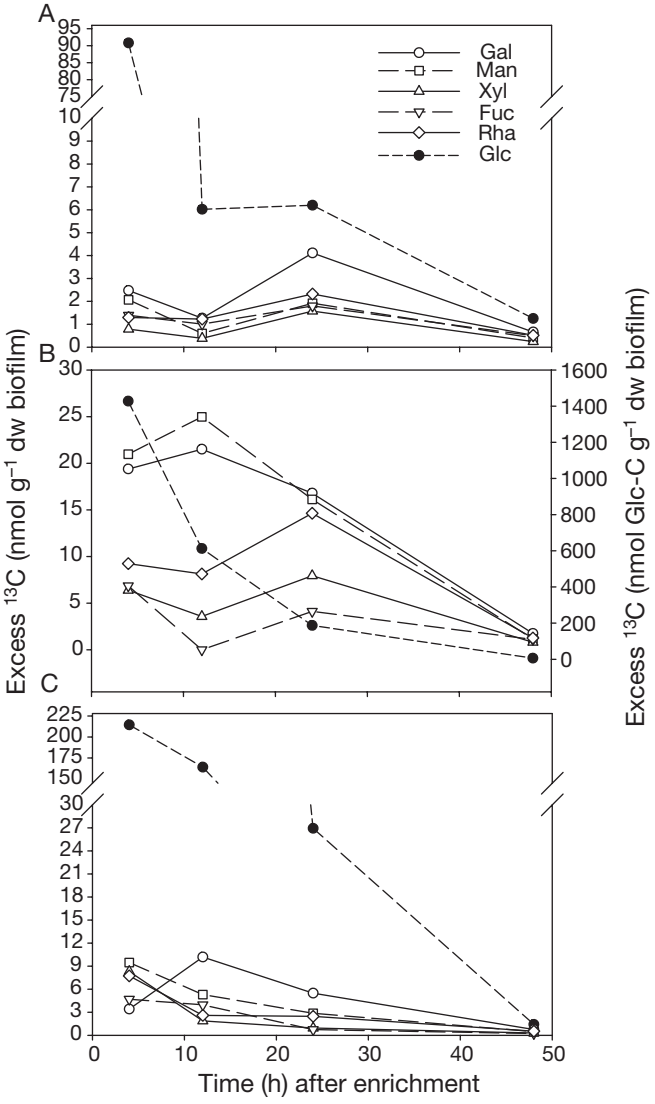

Fig. 4. Excess ^{13}C values of monosaccharides in hydrolyzates from (A) the colloidal carbohydrate fraction, (B) the hot-water soluble fraction, with glucose values on the right *y*-axis, and (C) the hot-bicarbonate soluble fraction (n = 1 for monosaccharides). See Table 1 for abbreviations

creased again after 24 h (Fig. 4A). Xylosyl residues displayed the lowest rate of isotopic depletion during the experiment, followed by Rha and Fuc (Table 2).

In the colloidal fraction, maximum isotopic enrichment of the majority of glycosyl residues occurred at 4 h and declined dramatically by 12 h (Table 2, Fig. 4B). At 4 h, incorporation of ^{13}C into glycosyl residues peaked, while the opposite was true for Xyl residues (Fig. 4B). The general pattern (with the exception of Glc) was that glycosyl residues were more enriched at 24 h than at 4 h (Fig. 4B). Glycosyl units that displayed comparatively slower rates of isotopic depletion over time included Xyl, Rha, and Fuc (Table 2, Fig. 4B).

Labeling patterns in the HB fraction were similar to that of the HW fraction (Table 2), although HB saccharides were not as enriched as those of the HW fraction at any time point (Fig. 4C). Maximal excess ^{13}C-values for most saccharide residues were observed after 4 h, with the exception of Gal, which peaked after 12 h (Fig. 4C). After 48 h, all monosaccharides in the HB fraction had excess ^{13}C-values <1 nmol ^{13}C g^{-1} dw biofilm, similar to results for the colloidal fraction (Fig. 4B,C).

In all polymer fractions, neutral sugars are only a component of the overall matrix. As such, the relative proportion of ^{13}C accounted for in the neutral sugar analysis was between 5 and 20% of the total ^{13}C content observed for a bulk polymer fraction. The total amount of ^{13}C measured for all neutral sugar fractions ranged from an initial high of ~3 µmol ^{13}C g^{-1} dw biofilm, with the HW fraction representing ~75% after 4 h, to <1 µmol ^{13}C g^{-1} dw biofilm after 48 h, the HB fraction containing ~33% of the ^{13}C measured in the neutral saccharides at this time point.

Isotopic analysis — PLFAs

Preliminary analysis of the total extracted neutral and glycolipid fractions from enriched sediments showed isotopic enrichment after 4 h (data not shown). Phospholipids were highly labeled while the neutral lipids were the least enriched of the 3 lipid fractions. The overall ^{13}C enrichment of an individual PLFA in the labeled samples was generally not as great as in individual sugars from the polysaccharide fractions (Table 3), but the ^{13}C-enrichment treatment still resulted in a 5- to 10-fold increase in δ^{13}C values in PLFAs compared to the controls. The total amount of ^{13}C recovered for all PLFAs was between 250 and 350 nmol ^{13}C g^{-1} dw biofilm, greater than what has been observed in terrestrial labeling experiments (Moore-Kucera & Dick 2008), but is likely similar to estimates of Veuger et al. (2006), where ^{13}C recovery in bacterial PLFA recovery was estimated at 107 nmol ^{13}C g^{-1} dw biofilm.

Content of ^{13}C in the PLFAs relative to neutral saccharides was very low initially (~12% of the recovered ^{13}C after 4 h), but increased after 48 h to ~43% of the recovered ^{13}C. The PLFA with the greatest labeling was 18:2ω6, a marker that can be found in cyanobacteria and green algae, with peak enrichment after 12 h (Table 3). However, the relative abundance of this lipid within the biofilms was less than 1%, indicating an overall small contribution to the carbon pool. PLFAs recognized as biomarkers for diatoms (20:5ω3,

Table 3. $\delta^{13}C$ (‰) isotopic values for all PLFAs from control and enriched plots from Alresford Creek, UK. 'General' PLFAs are non-specific to a functional group. Where SD given, n = 2

	PLFA	Control			Enriched		
		Time (h) after enrichment			Time (h) after enrichment		
		12	24	48	4	12	24	48
Prokaryotes								
General	14:0	234.9 ± 62.7	9.9 ± 2.5	1.8 ± 3.6	1878.9 ± 62.9	2712.1 ± 106.4	2366.2 ± 884.9	1501.8 ± 596.6
	15:0	91.7 ± 19.0	–2.6 ± 1.4	–6.7 ± 0.9	455.6 ± 136.3	738.6 ± 33.0	894.2 ± 159.5	748.7 ± 275.3
	16:0	173.8 ± 40.7	8.1 ± 0.2	–2.8 ± 2.9	1692.9 ± 251.6	2576.8 ± 32.7	1961.5 ± 694.6	1233.1 ± 439.7
	16:1ω7	157.0 ± 35.5	0.3 ± 2.1	–9.7 ± 2.0	1227.7 ± 22.7	2092.9 ± 146.3	1917.2 ± 661.2	1375.5 ± 428.9
	17:0	55.7 ± 12.6	–6.9 ± 7.0	–10.7 ± 3.2	282.4	402.7 ± 237.5	601.5 ± 196.9	422.4 ± 128.9
	17:1ω7	46.0 ± 13.9	–7.5 ± 0.3	–11.5 ± 0.1	222.6	290.5 ± 17.5	675.2 ± 76.4	519.8 ± 180.8
	18:0				344.3 ± 43.5	445.0 ± 17.2	397.1 ± 142.0	400.8 ± 165.9
Gram-positive bacteria	i14:0[a]	65.5 ± 8.4	2.0 ± 2.9	–9.5 ± 0.9	115.6	207.8 ± 21.9	603.4 ± 296.5	891.7 ± 364.1
	i15:0[a]	58.8 ± 18.7	–12.8 ± 5.0	–39.4 ± 0.8	324.5 ± 105.7	452.6 ± 1.8	932.2 ± 391.2	676.0 ± 323.3
	a15:0[a]	32.8 ± 3.4	–6.3 ± 0.9	–14.5 ± 0.7	132.3 ± 25.2	221.6 ± 34.5	479.8 ± 158.5	454.2 ± 206.5
	i16:0[a]							
Gram-negative bacteria	18:1ω7[b]	64.5 ± 25.4	–4.0 ± 1.0	–11.3 ± 0.1	400.2 ± 149.2	723.1 ± 7.9	688.7 ± 190.3	651.1 ± 314.9
	cy19:0[e]				521.7	378.8 ± 38.1	201.8 ± 76.9	
Eukaryotes								
General	16:0	173.8 ± 40.7	8.1 ± 0.2	–2.8 ± 2.9	1692.9 ± 251.6	2576.8 ± 32.7	1961.5 ± 694.6	1233.1 ± 439.7
	18:1ω12	65.2 ± 19.5	–3.0 ± 1.1	–10.3 ± 0.8				
	18:3ω3[d]			–11.2 ± 2.2	524.6			330.3 ± 146.5
	18:2ω6				3117.2	3971.5 ± 886.7	1152.2 ± 523.4	608.4 ± 210.1
	20:1ω9	21.8 ± 18.2	–9.1 ± 0.8	–10.8 ± 1.2	115.6	448.7	210.1 ± 101.4	249.9 ± 100.6
	20:2ω7		–7.3 ± 1.7			34.6	–0.8 ± 35.4	
	20:2ω9	44.6 ± 27.2	–8.0 ± 1.1	–11.6 ± 0.7		30.1	–0.8 ± 35.4	–18.2
	20:4ω6				437.7	1212.8 ± 152	439.3 ± 166.9	215.8 ± 75.9
	22:1ω10	36.9 ± 18.1	–12.7 ± 1.3	–13.8 ± 0.7				
	24:0	146.5 ± 28.8	8.5 ± 2.4	9.0 ± 5.9	1676.5	5831.5 ± 1101.5	4157.5 ± 1412.7	2236.8 ± 698.4
	16:2ω4[c]					592.6	885.5	447.5
Diatom	20:5ω3[c]	42.8 ± 30.1	–11.2 ± 3.6	–12.3 ± 1.9	248.5 ± 16.6	638.4 ± 158.5	297.8 ± 136.9	287.1 ± 114.3
	22:6ω3[c]	25.1 ± 30.3	–12.5 ± 2.4	–11.3 ± 0.8	127.16	256.1 ± 77.9	120.1 ± 65.1	102.4 ± 17.4

[a]Gram-positive bacteria, [b]Gram-negative bacteria, [c]diatoms, [d]green algae, [e]stress PLFA produced by Gram-negative bacteria

16:2ω4, and 22:6ω3) showed enrichment over the study period (Table 3 lists all of the PLFA $\delta^{13}C$-values measured). The primary marker 20:5ω3 had the highest enrichment of all diatom PLFAs, and maximal values were recorded at 12 h (Table 3, Fig. 5A). Overall, excess ^{13}C-values for diatom PLFAs changed little between 24 and 48 h (Fig. 5A), indicating the persistence of diatoms through time and that enriched lipids were being produced by the diatoms from an enriched carbon source through time (van Oevelen et al. 2006a).

The Gram-positive bacterial PLFA biomarkers i14:0, i15:0, and a15:0 each showed a general pattern of increased ^{13}C-labeling throughout the study period (Table 3, Fig. 5B) with only a small decline in excess ^{13}C observed for i15:0 and a15:0 after 48 h (Fig. 5B). Excess ^{13}C-values for i14:0 steadily increased throughout the sampling period, peaking after 24 h, and only declining slightly after 48 h (Fig. 5B). Cy19:0 was the only bacterial biomarker to show maximum labeling at 4 h and declined thereafter (Table 3). Significant labeling was found in the Gram-negative bacterial PLFA 18:1ω7, where labeling peaked after 24 h before declining slightly after 48 h (Fig. 5A). The proportion of ^{13}C incorporated into the main bacterial and diatom biomarkers relative to the total PLFA pool was relatively consistent through time at ~13%, with Gram-negative bacteria having the largest amount of ^{13}C present (5 to 7% of the total ^{13}C in the PLFAs), followed by diatoms (Fig. 6A).

The biosynthesized compound pools measured here (PLFAs, bulk polymer fractions and their neutral sugars) resulted in recovery of ~20 µmol ^{13}C g^{-1} dw biofilm after 4 h, declining to ~5 µmol ^{13}C g^{-1} dw biofilm after 2 d, primarily due to the loss of ^{13}C from the polymer (EPS, chrysolaminaran) pools

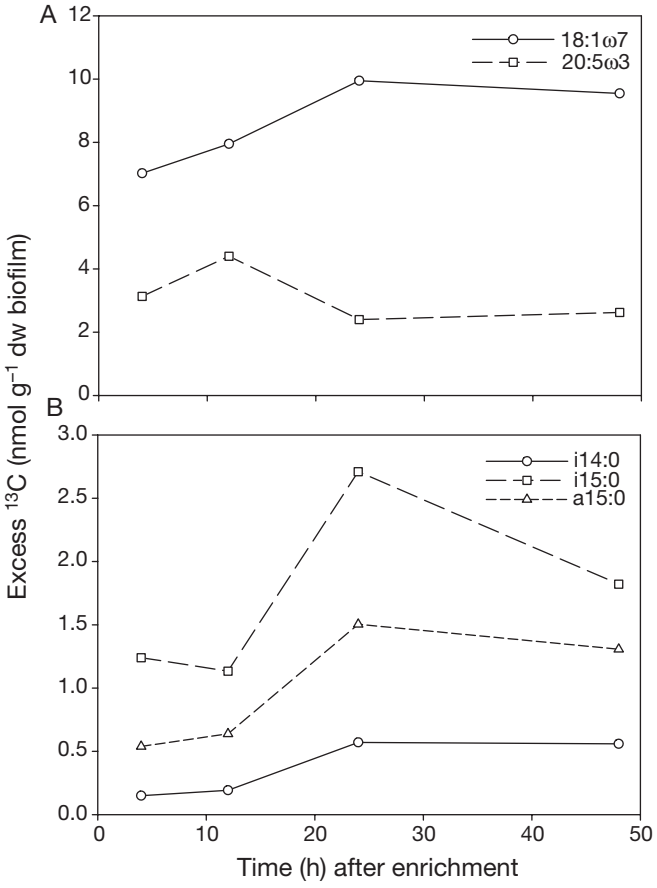

Fig. 5. Excess ^{13}C values of PLFAs diagnostic for (A) diatoms (20:5ω3) and Gram-negative bacteria (18:1ω7), and (B) Gram-positive bacteria (a15:0, i15:0, i14:0)

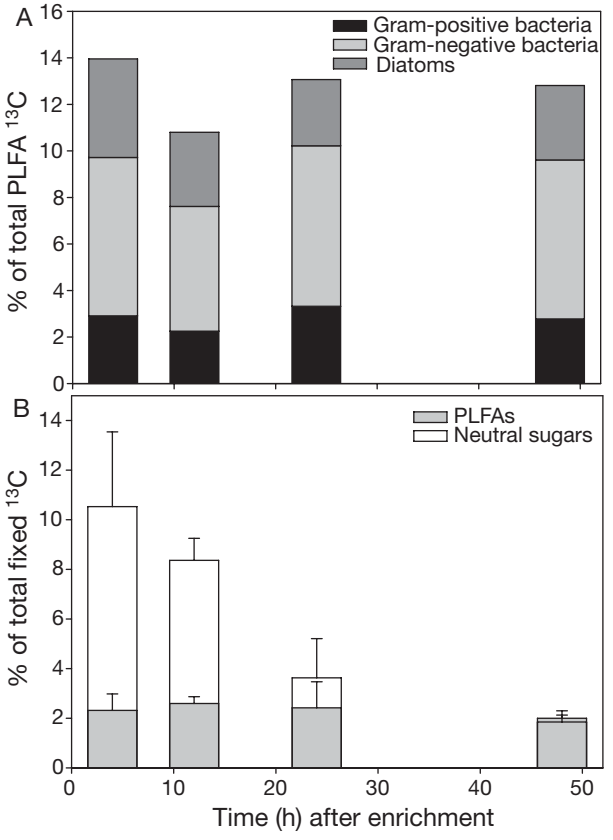

Fig. 6. Recovery of ^{13}C into (A) bacterial and diatom PLFAs relative to the total amount of ^{13}C measured in all PLFAs, and (B) neutral sugars (sum of all extracted fractions) and total PLFAs as a proportion of the total fixed ^{13}C in the biofilm (n = 3)

(~85% of the ^{13}C in the polymer fractions was lost after 2 d). Recovery of the total ^{13}C fixed by the biofilms into polymer neutral sugars and PLFAs peaked after 4 h with approximately 16% recovery, declining to ~4% at the end of the study period (Fig. 6B). The bulk of this ^{13}C was found in the neutral sugars (~14% after 4 h), with the PLFAs maintaining a fairly constant percentage of the fixed ^{13}C pool over the observation period. By the end of the study period, both the neutral sugars and PLFAs contained 2% of the estimated total ^{13}C fixed in the biofilms (Fig. 6B).

DISCUSSION

Conceptual model of C flow within diatom-dominated estuarine mudflat biofilms

Benthic epipelic diatoms are one of the primary sources of EPS within estuarine biofilms (Underwood & Paterson 2003). We used an *in situ* carbon pulse-chase approach to track autotrophic C-fixation and production of polysaccharides and PLFAs and the flow of isotopically enriched carbon within the bacterial community over 48 h. Isotopic enrichment of the overall algal community was significant (Table 3), with substantial photosynthetic uptake of ^{13}C-labeled bicarbonate by the biofilm community (top 2 mm of the sediment) during the low tide period resulting in incorporation (within 4 h) of ^{13}C into diatom intracellular storage carbohydrates, extracellular polysaccharides, and into PLFAs (Tables 2, 3, Fig. 6B). These data demonstrate various possible routes for the flow of carbon between autotrophs and heterotrophic bacteria and the significance of carbohydrates produced by diatoms in this exchange. Measuring the isotopic enrichment of saccharides from diatom-derived polymers builds on the results of Hanlon et al. (2006) allowing a conceptual model of the role of EPS in biofilm carbon flow to be expanded (Fig. 7).

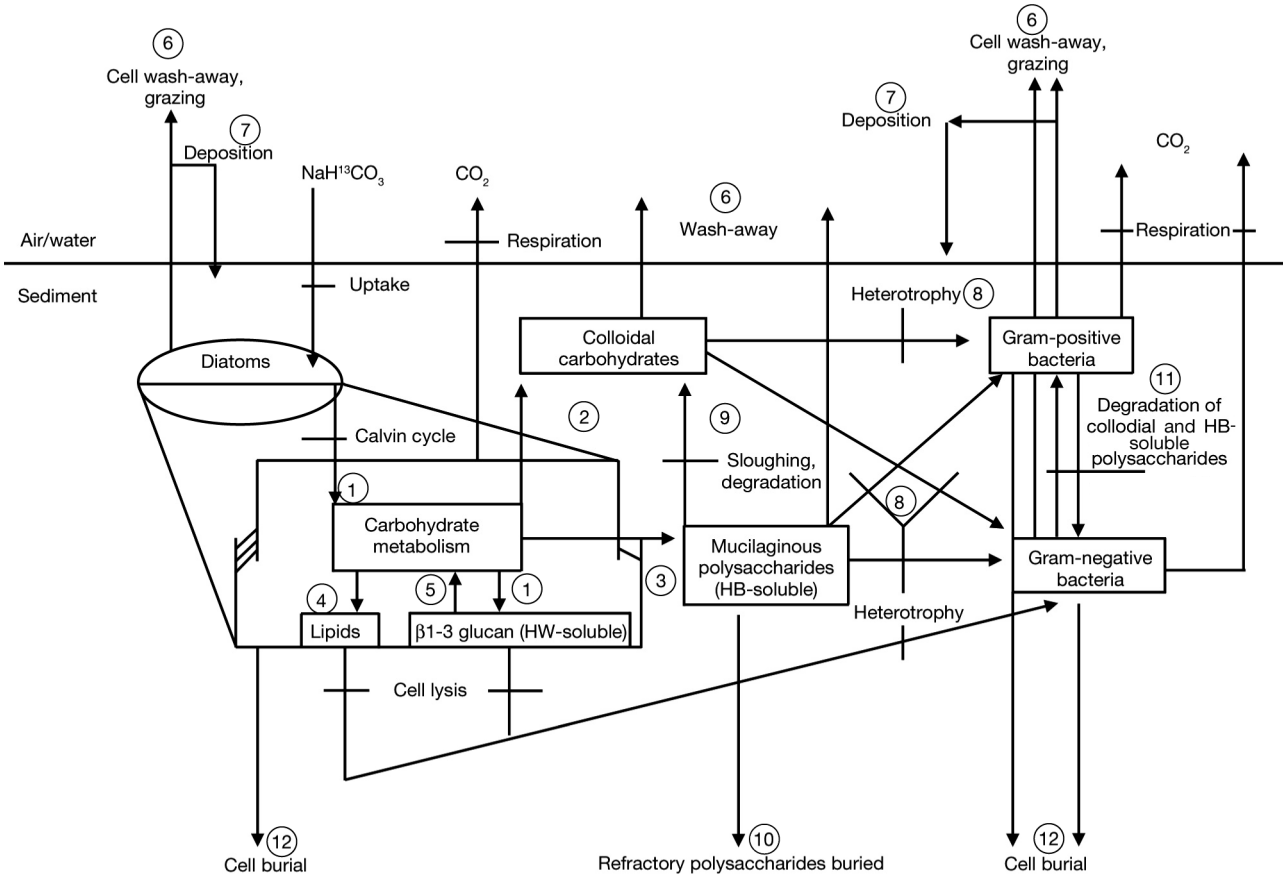

Fig. 7. Conceptual model of the flow of carbon after uptake by diatoms. The model is a compilation of events over multiple tidal cycles in a typical diatom-dominated biofilm. HW: hot-water, HB: hot-bicarbonate. Numbers correspond to events described in the text: (1) uptake of carbon and partitioning into chrysolaminaran; (2) colloidal carbohydrate production; (3) capsular (HB soluble) carbohydrate production; (4) lipid production; (5) catabolism of chrysolaminaran and respiration; (6) cell and polymer wash-away; (7) cell deposition; (8) utilization of extracellular polysaccharides by bacteria; (9) link between mucilaginous and colloidal polysaccharides; (10) accumulation of refractory portions of the mucilaginous polysaccharide; (11) recycling of carbon between Gram-negative and Gram-positive bacteria and with diatoms; and (12) cell burial

Production and fate of diatom polysaccharides

Glucose, initially the most isotopically enriched monosaccharide residue in the present study (Fig. 7-1), is a key component of intra- and extracellular polysaccharides produced by diatoms (Hoagland et al. 1993, Underwood & Paterson 2003, Chiovitti et al. 2004) and appears to have played a central role in the exchange of C within autotroph metabolism, with implications for heterotrophic utilization in these biofilms. The delay in the maximal ^{13}C enrichment in the diatom PLFA 20:5ω3 (Fig. 5a) relative to glucosyl residues (Fig. 4a) points to the rapid production and utilization of chrysolaminaran, the persistence of this intracellular storage compound over an extended period of time, and the importance of diatom storage polysaccharides in fueling metabolic processes within these biofilms. Initially, fixed carbon was preferentially used for chrysolaminaran production (Figs. 4 & 7-1), but was also used by cells for the production of EPS when illuminated (Fig. 7-2,-3). The rate of EPS production by diatom biofilms during tidal exposure periods is affected by endogenous rhythms, light levels, and nutrient status (Smith & Underwood 1998, Underwood & Paterson 2003, Hanlon et al. 2006). While excess EPS can be produced when cells are light-stressed and nutrient-limited (sometimes referred to the as 'overflow hypothesis'), the available nutrient data and the observation that most ^{13}C label was initially found in intracellular glucan indicate that 'overflow' was not a major component of EPS production in this experiment. Previous diel studies have shown that the relative abundance of glucose in the HW fraction increases during a daytime emersion period (Hama & Handa 1992, Hanlon et al. 2006), and the majority of the glucosyl units are components of the storage polymer chrysolaminaran, composed of (1 → 3) β-glucan chains (Chiovitti et al. 2004, Abdullahi et al. 2006). Isotopic labeling patterns of

chrysolaminaran observed here are in agreement with ^{14}C-labeling of benthic biofilms (Smith & Underwood 1998) and ^{13}C-labeling of phytoplankton (Hama & Handa 1992), where the bulk of isotopic enrichment was found in intracellular glucan over short time periods. Utilization of chrysolaminaran can be rapid and significant in the dark (Smith & Underwood 1998), and our data show that enriched glucan within the HW fraction was not completely utilized/diluted over a 48 h period (Fig. 7-5). While isotopically enriched chrysolaminaran was used for the production of PLFAs and EPS (discussed below; Fig. 7-5), the intracellular chrysolaminaran pool of diatoms does not appear to be completely turned over during a single (6 to 12 h) dark period (Smith & Underwood 1998).

HW extraction may result in incomplete solubilization of chrysolaminaran, with the remaining glucan solubilized during the subsequent HB extraction step (Hama & Handa 1992, Abdullahi et al. 2006), which would explain the similar patterns in the relative abundance and isotopic enrichment of glucose observed in the HB and HW fractions in the present study. In addition to extraction of chrysolaminaran, HW has been shown to partially extract extracellular polysaccharides from phytoplankton (Hama & Handa 1992), and also from marine and freshwater diatoms (Chiovitti et al. 2004, Abdullahi et al. 2006), accounting for the smaller proportions of non-glucose monosaccharide residues detected in the HW fraction.

Cell–cell and cell–substratum interactions are facilitated by the production of tightly bound (HB soluble) carbohydrates (Fig. 7-3; Wang et al. 1997, Wustman et al. 1997, Chiovitti et al. 2003a). While the HB fraction is primarily diatom-derived (Bellinger et al. 2005, Abdullahi et al. 2006), HB content in the present study was not correlated with chl *a*, consistent with previous diel observations from the Colne Estuary (Hanlon et al. 2006), indicating that the HB content was uncoupled from the diatom biomass at some point. The HB fraction, once secreted, can become an integral part of the biofilm matrix and is likely a primary factor in biostabilization processes based on its structural complexity and potential for being highly refractory (Wustman et al. 1997, Chiovitti et al. 2003a, Abdullahi et al. 2006). This long-term persistence may explain why the HB fraction does not closely correlate with diatom biomass. Further work to understand the biochemistry and physical nature of these polysaccharides within the HB fraction is required.

The patterns in isotopic enrichment of individual monosaccharide residues provided some clues as to the organization and synthesis of mudflat biofilm polymers by indicating which residues were actively incorporated into polymers at a particular time, and which were more or less susceptible to degradation. The most abundant saccharides detected, i.e. glucose, mannose, xylose, and galactose, were also the most highly ^{13}C-labeled (Tables 1 & 2). These glycosyl residues have been found to be important constituents in diatom extracellular polysaccharides (Hoagland et al. 1993, Wustman et al. 1998, Chiovitti et al. 2003a). In the present study, labeled xylosyl, rhamnosyl, and fucosyl residues exhibited a slower rate of decline in isotopic enrichment relative to glucosyl, galactosyl, and mannosyl residues, indicating accumulation within the biofilm over time (Table 2, Fig. 4). These changes are indicative of varied turnover times of different saccharides within the intertidal sediment carbohydrate pool, and are in general agreement with changes observed over short-term laboratory degradation studies conducted on sediment slurries (Hofmann et al. 2009). In peat sediments, xylose and rhamnose accumulate with depth relative to hexoses (Macko et al. 1990), while deoxy sugar-containing regions of polymers produced by a planktonic diatom tend to be more resistant to degradation, as hexose-rich polymers are more rapidly degraded by bacteria (Skoog & Benner 1997, Giroldo et al. 2003). Persistence of deoxy sugars and pentoses will result in greater hydrophobicity of the biofilm (Zhou et al. 1998), thereby increasing biostabilization potential. Uronic acid residues also have the potential to increase cell–substratum interactions through cationic cross-linking. Analysis of fractions here (Fig. 2C) and in culture studies (Hoagland et al. 1993, Wustman et al. 1997, Hanlon et al. 2006) have found uronic acids to be a significant component of EPS fractions (25 to 65% w:w of a fraction; McConville et al. 1999, Underwood et al. 1995). The isotopic signature of uronic acids was not determined here, but their abundance within the fractions may account for some of the differences observed between bulk fraction signatures (Fig. 3) and the results observed for the individual neutral sugars (Table 2). The presence of proteins in EPS (Chiovitti et al. 2003b) may also account for additional C-stores within diatom-produced polymers and will further influence functional roles within the biofilm matrix.

Rapid and continuous production of EPS (colloidal and HB fractions) from a ^{13}C-labeled carbon source through time was evident, even after the removal of inorganic ^{13}C by subsequent tides. However, the relationship with algal biomass and functional roles within the sediments appear to differ for the colloidal and HB carbohydrate fractions based on differences in carbohydrate content and biochemistry (de Brouwer & Stal 2001, Underwood & Paterson 2003, Abdullahi et al. 2006). The loss of approximately 60% of the colloidal carbohydrate content (Hanlon et al. 2006), or the resuspension of up to 50% of the MPB during high tide (de Jonge & van Beusekom 1992) are sources of carbon

loss from the sediment surface (Fig. 7-6). Colloidal carbohydrates were significantly correlated with estimated algal biomass over the study period for all samples (Fig. 2; see also Underwood & Smith 1998, Taylor et al. 1999, Lucas et al. 2003). Wash-away of the bulk of the colloidal carbohydrate fraction was evidenced by the large declines in saccharide isotopic enrichment after the first tidal cycle. However, despite large losses of the colloidal carbohydrate fraction during each subsequent high tide period, continued isotopic enrichment of this labile pool indicates new production from an enriched, possibly intracellular carbon source (i.e. chrysolaminaran) or extracellular (i.e. HB) carbon source. The production of 'new' ^{13}C-labeled colloidal carbohydrate from an enriched carbon source, including material derived from the sloughing or degradation of more refractory, tightly bound polymer (i.e. the HB fraction; Underwood & Paterson 2003, Bellinger et al. 2005), was evidenced by the second spike in isotopic enrichment of saccharides such as galactose from the colloidal carbohydrate fraction at 24 h (Fig. 4). While colloidal carbohydrates are rich in carbon and therefore metabolically expensive to produce, the labile and soluble nature of the colloidal fraction is a reflection of the biochemistry of these polymers, either inherently during production or through microbial alteration.

Bacterial degradation of diatom-derived polysaccharides

The activity of heterotrophic Gram-negative bacteria in polymer degradation (Fig. 7-8) was likely balanced by the continuous production of mucilaginous (HB-soluble) polysaccharides by diatoms in these biofilms (Fig. 7-3). Cook et al. (2007) have shown the significant release of organic carbon (primarily as EPS) under nutrient-limited and -replete conditions, the bulk of which is used by the microbial community. Extracellular β-glucosidase activity has been correlated with both EPS and HB carbohydrate content in slurry experiments (Haynes et al. 2007). A balance between production and utilization of these matrix polysaccharides would explain the near static carbohydrate content, while the declining ^{13}C signal measured over time suggests a turnover of the individual polymers relative to production in the HB fraction (Figs. 2 & 3). The significance of Gram-negative bacteria in carbon flow dynamics within these surface biofilms was evident from the abundance and ^{13}C-enrichment of 18:1ω7 observed (Table 3; see also Middelburg et al. 2000). Gram-negative bacteria were found to have some of the largest isotopic enrichments observed (Fig. 5), a result of their rapid utilization (Haynes et al. 2007, Hofmann et al. 2009) of the initial rapid expulsion of ^{13}C-enriched LMW and EPS photosynthate excreted fairly quickly after photoassimilation by diatoms (Smith & Underwood 1998, Middelburg et al. 2000, de Brouwer & Stal 2001) and the continued production of EPS from ^{13}C-enriched intracellular carbon stores. Algae have been found to allocate a large proportion of photosynthate into polysaccharides (up to 70%; Wainman et al. 1999; Wolfstein et al. 2002) and proteins, while a smaller proportion is used for lipid production (as little as 10%; Wainman et al. 1999). Our findings confirm that a smaller proportion of carbon was used by diatoms for lipid production (Fig. 5a), and a large amount was exuded as EPS, providing a large C-source for the Gram-negative bacterial community, as evidenced by the significantly greater enrichment of the PLFA 18:1ω7 (Fig. 5a; Middelburg et al. 2000, Veuger et al. 2006). Gram-negative bacteria are a prominent component in biofilm communities in other muddy as well as sandy estuarine biofilms (Middelburg et al. 2000, Bühring et al. 2005, Cook et al. 2007), where members of the subphyla *Flavobacteria* and *Sphingobacteria* (previously *Cytophaga–Flexibacter–Bacteroides*) and of the *Alpha-* and *Gammaproteobacteria* have been identified as key bacterial taxa involved in carbohydrate turnover (Haynes et al. 2007). Bühring et al. (2005) observed a large Gram-negative bacterial component in biofilms primarily from the *Cytophaga–Flavobacterium* group, which are well known degraders of complex biopolymers.

Heterotrophic degradation of biofilm polymers in the present study appeared to have occurred both directly and indirectly through subsequent turnover or recycling of microbial carbon. Giroldo et al. (2005) noted a 2-step degradation process of EPS from HMW to LMW polymers and subsequent utilization of LMW compounds. In the present study, isotopic label differentially accumulated within the Gram-negative and Gram-positive bacterial community, indicating that these groups were not only utilizing diatom-derived EPS, but were also turning over carbon with the microbial pool (Fig. 7-11). Recycling of bacterial carbon to the dissolved organic carbon pool has been found to be high (72% of C produced), and bacterial carbon can be subsequently degraded, maintaining a relatively enriched carbon source within sediments for an extended period of time (van Oevelen et al. 2006a). The persistent and increasing enrichment of bacterial PLFA biomarkers would support the argument that these organisms are not only continuing to utilize diatom-derived EPS, but are also using heterotrophically processed ^{13}C (Fig. 6A).

Persistence of diatoms within biofilms

Despite the variety of factors that could result in the removal of diatoms or bacteria from the top few mm of

the sediment surface (e.g. burial, grazing, wash-away; Fig. 7-6, -12), it was apparent that these cells can persist within an area over an extended period of time. Such persistence may be closely linked to the integrity of the biofilm due to EPS (Underwood & Paterson 2003). Isotopic enrichment of the diatom PLFA 20:5ω3 over 48 h indicates that enriched diatom cells remained within the study area over multiple tidal cycles despite declines in algal biomass (chl *a*) due to wash-away or grazing by the gastropod *Hydrobia ulvae* (Fig. 1B).

Isotopic enrichment of PLFAs, albeit small, within the control cores was also observed, notably after the first tidal cycle (12 h) following initial enrichment of treatment plots. This observation suggests that small-scale movements of enriched organisms out of the enriched area occurred during high tide through re-suspension and rapid deposition. The 'turbid tidal edge' of the incoming tide wave coving a mudflat picks up material but rapidly drops large flocs out of suspension (Hanlon et al. 2006). The duration of suspension is dependent on the chemistry of the polymers associated with the cells (Fig. 7-7). Increased floc formation and sedimentation of algal cells has been attributed to increased deoxysugar content (Giroldo et al. 2003), and the sedimentation of polysaccharides can increase sediment carbohydrate content upwards of 30% (Hanlon et al. 2006). In the present study, the relative proportion of deoxysugar residues within the colloidal and HB fractions ranged from 7 to 20% of the total detected sugar content, contributing a significant hydrophobic component to the diatom exudates and increasing the probability of floc formation and cell deposition.

Significance of autotrophic polymers and their use by heterotrophs in biofilms

The variability found in the patterns of labeling between diatom PLFAs and the individual saccharide residues in polymers of each fraction highlights the benefits of simultaneously tracking isotopes in multiple biomolecules (Veuger et al. 2006, Cook et al. 2007). Analysis of PLFAs or bulk carbohydrate fractions in isolation would have led to a different interpretation and an incomplete understanding of the movement of carbon through specific saccharides within each polymer pool. The large excess ^{13}C-values measured for the glycosyl residues from each fraction indicated that a significant component of carbon fixed by diatoms was sequestered within polysaccharides, reflecting the importance of these materials within the biofilm matrix. Differential labeling of the bacterial PLFAs demonstrated the varied responses of the microbial community to the substrates available to them. Boschker et al. (1998) showed that addition of a labile carbon source (e.g. acetate) will initially result in labeling of PLFAs within a microbial community as a result of specific uptake. Moore-Kucera & Dick (2008) noted very low recovery of ^{13}C in PLFAs where a poor quality substrate (Douglas-fir material) was added (~12 nmol ^{13}C-PLFA g^{-1} soil). In the present study, the diatom community was actively photosynthesizing and producing EPS, a higher quality carbon source; thus, the content of ^{13}C in the PLFAs was measured at upwards of 350 nmol ^{13}C-PLFA g^{-1} dw biofilm.

Once the carbon source is exhausted, subsequent labeling of other microbial PLFAs is a result of the utilization of microbial products (Ziegler et al. 2005). Addition of exogenous diatom EPS to biofilms has been found to selectively promote the growth of Gram-negative *Gammaproteobacteria*, particularly a species of *Acinetobacter*, rather than to stimulate the whole bacterial sediment assemblage (Haynes et al. 2007). In the present study, the Gram-positive bacteria did not utilize the initially-labeled carbon sources as readily as Gram-negative bacteria did. This indicates that groups of heterotrophicbacteria cannot necessarily access all of the different carbohydrate fractions within the biofilms. Culture experiments have shown that an estuarine *Varivorax* species can easily grow on colloidal EPS but not on HB-soluble polymers (Hofmann et al. 2009). The increasing ^{13}C enrichment in Gram-positive bacterial PLFAs observed in the present study is likely the result of a labile carbon source becoming more accessible to those bacteria over time due to coupled microbial dynamics and carbon cycling. Cycling of bacterially-derived ^{13}C-labeled-DOM or ^{13}C-labeled-DIC into diatoms also enhances isotopic enrichment over a longer time period (Veuger et al. 2006).

The carbohydrate polymer fractions studied here (colloidal, HW, and HB) constitute over 50% of the total sediment carbohydrate content (Bellinger et al. 2005) and contribute 30 to 50% of the total organic matter present in muddy surficial sediments. Isotopic analysis indicated that 5 to 20% of the ^{13}C incorporated in polymers could be found in the hydrolyzed neutral sugars of a bulk polymer fraction. Uronic acids were found here to constitute approximately 20% of a polymer fraction (Fig. 2C), although upwards of 65% of a fraction may be composed of uronic acids (Underwood et al. 1995). While proteins and lipids generally do not make up large proportions of diatom EPS (i.e. McConville et al. 1999, but see Chiovitti et al. 2003b), these additional carbon sinks in the extracted fractions would contribute to the differential labeling patterns measured. These results indicate that additional compounds should be measured, and the analytical procedures for neutral sugar analysis may also need to be modified to ensure complete hydrolysis while minimiz-

ing degradation. While a comprehensive carbon budget was not the explicit goal of this work, it is evident from our results that the EPS component of estuarine biofilms needs to be quantified when putting together budgets and models of C-flow within these highly dynamic communities. PLFAs have been used in carbon budgets, but the amount of ^{13}C found in the total PLFA pool relative to the amount of ^{13}C added to sediments may be as low as 0.1% (Moore-Kucera & Dick 2008), and our results indicate that diatom-synthesized polymers can contain upwards of 90% of the ^{13}C synthesized between these respective pools, confirming the significance of EPS not only as a resource for heterotrophs, but also as a significant carbon compound in estuarine biofilms.

Acknowledgements. We thank T. Hoffman, T. Cresswell-Maynard, and J. Green for their assistance in the field, and D. Lueking and the Stable Isotope Lab at the University of Arkansas for their assistance with the PLFAs. We also thank J. Middelburg and E. Boschker for their thoughtful discussions, comments, and suggestions, which led to improvements in this manuscript. This work was funded by National Science Foundation grants IBN-0110875 awarded to M.R.G. and G.J.C.U., DEB-0445357 to S.E.Z., and UK NERC grant NER/A/S2001/ 00536 awarded to G.J.C.U., A. S. Ball, and A. M. Osborn.

LITERATURE CITED

Abdullahi AS, Underwood GJC, Gretz MR (2006) Extracellular matrix assembly in diatoms (Bacillariophyceae). V. Environmental effects on polysaccharide synthesis in the model diatom, *Phaeodactylum tricornutum*. J Phycol 42: 363–378

Abrajano Jr TA, Murphy DE, Fang J, Comet P, Brooks JM (1994) $^{13}C/^{12}C$ ratios in individual fatty acids of marine mytilids with and without bacterial symbionts. Org Geochem 21:611–617

Amon RMW, Benner R (1996) Bacterial utilization of different size classes of dissolved organic matter. Limnol Oceanogr 41:41–51

Apoya-Horton MD, Liang Y, Underwood GJC, Gretz MR (2006) Movement modalities and responses to environmental changes of the mudflat diatom *Cylindrotheca closterium* (Bacillariophyceae). J Phycol 42:379–390

Arnosti C, Repeta DJ (1994) Oligosaccharide degradation by anaerobic marine bacteria: characterization of an experimental system to study polymer degradation in sediments. Limnol Oceanogr 39:1865–1877

Bellinger BJ, Abdullahi AS, Gretz MR, Underwood GJC (2005) Biofilm polymers: relationship between carbohydrate biopolymers from estuarine mudflats and unialgal cultures of benthic diatoms. Aquat Microb Ecol 38: 169–180

Boschker HTS, Middelburg JJ (2002) Stable isotopes and biomarkers in microbial ecology. FEMS Microbiol Ecol 40: 85–95

Boschker HTS, Nold SC, Wellsbury P, Bos D, de Graaf W, Pel R, Parkes RJ, Cappenberg TE (1998) Direct linking of microbial populations to specific biogeochemical processes by ^{13}C-labelling of biomarkers. Nature 392: 801–805

Boschker HTS, Kromkamp JC, Middelburg JJ (2005) Biomarker and carbon isotopic constraints on bacterial and algal community structure and functioning in a turbid, tidal estuary. Limnol Oceanogr 50:70–80

Bühring SI, Elvert M, Witte U (2005) The microbial community structure of different permeable sandy sediments characterized by the investigation of bacterial fatty acids and fluorescence in situ hybridization. Environ Microbiol 7:281–293

Chiovitti A, Higgins MJ, Harper RE, Wetherbee R (2003a) The complex polysaccharides of the raphid diatom *Pinnularia viridis* (Bacillariophyceae). J Phycol 39:543–554

Chiovitti A, Bacic A, Burke J, Wetherbee R (2003b) Heterogeneous xylose-rich glycans are associated with extracellular glycoproteins from the biofouling diatom *Craspedostauros australis* (Bacillariphyceae). Eur J Phycol 38: 351–360

Chiovitti A, Molino P, Crawford SA, Teng R, Spurck T, Wetherbee R (2004) The glucans extracted with warm water from diatoms are mainly derived from intracellular chrysolaminaran and not extracellular polysaccharides. Eur J Phycol 39:117–128

Cloern JE, Canuel EA, Harris D (2002) Stable carbon and nitrogen isotope composition of aquatic and terrestrial plants of the San Francisco Bay estuarine system. Limnol Oceanogr 47:713–729

Cook PLM, Veuger B, Böer S, Middelburg JJ (2007) Effect of nutrient availability on carbon and nitrogen incorporation and flows through benthic algae and bacteria in near-shore sandy sediment. Aquat Microb Ecol 49:165–180

de Brouwer JFC, Stal LJ (2001) Short-term dynamics in microphytobenthos distribution and associated extracellular carbohydrates in surface sediments of an intertidal mudflat. Mar Ecol Prog Ser 218:33–44

Decho AW (2000) Microbial biofilms in intertidal systems: an overview. Cont Shelf Res 20:1257–1273

de Jonge VN, van Beusekom JEE (1992) Contribution of resuspended microphytobenthos to total phytoplankton in the Ems Estuary and its possible role for grazers. Neth J Sea Res 30:91–105

Dunstan GA, Volkman JK, Barrett SM, Leroi JM, Jeffrey SW (1994) Essential polyunsaturated fatty acids from 14 species of diatom (Bacillariophyceae). Phytochemistry 35: 155–161

Eaton JW, Moss B (1966) The estimation of numbers and pigment content in epipelic algal populations. Limnol Oceanogr 11:584–595

Findlay RH (2007) Determination of microbial community structure using phospholipid fatty acid profiles. In: Kowalchuk GA, de Bruijin FJ, Head IM, Akkermans AD, van Elsas JD (eds) Molecular microbial ecology manual. Kluwer Academic Publishers, Dordrecht, p 983–1004

Findlay RH, Trexler MB, Guckert JB, White DC (1990) Laboratory study of disturbance in marine sediments: response of a microbial community. Mar Ecol Prog Ser 62:121–133

Flora JW, Null AP, Muddiman DC (2002) Dual-micro-ESI source for precise mass determination on a quadrupole time-of-flight mass spectrometer for genomic and proteomic applications. Anal Bioanal Chem 373:538–546

Fry B, Sherr EV (1984) ‰^{13}C measurements as indicators of carbon flow in marine and freshwater ecosystems. Contrib Mar Sci 27:13–47

Giroldo D, Vieira AAH, Paulsen BS (2003) Relative increase of deoxy sugars during microbial degradation of an extracellular polysaccharide released by a tropical freshwater *Thalassiosira* sp. (Bacillariophyceae). J Phycol 39: 1109–1115

Giroldo D, Vieira AAH, Paulsen BS (2005) Extracellular polysaccharides produced by a tropical cryptophyte as a carbon source for natural bacterial populations. Eur J Phycol 40:241–249

Goes JI, Handa N, Taguchi S, Hama T, Saito H (1996) Metabolism of neutral monosaccharide constituents of storage and structural carbohydrates in natural assemblages of marine phytoplankton exposed to ultraviolet radiation. Limnol Oceanogr 41:1478–1489

Hama J, Handa N (1992) Diel variation of water-extractable carbohydrate composition of natural phytoplankton populations in Kinu-ura Bay. J Exp Mar Biol Ecol 162:159–176

Hanlon ARM, Bellinger B, Haynes K, Xiao G and others (2006) Dynamics of extracellular polymeric substance (EPS) production and loss in an estuarine, diatom-dominated, microalgal biofilm over a tidal emersion-immersion period. Limnol Oceanogr 21:79–93

Haynes K, Hofman TA, Smith CJ, Ball AS, Underwood GJC, Osborn AM (2007) Diatom-derived carbohydrates as factors affecting bacterial community composition in estuarine sediments. Appl Environ Microbiol 73:6112–6124

Hedges JI, Stern JH (1984) Carbon and nitrogen determinations of carbonate-containing soils. Limnol Oceanogr 29: 657–663

Hoagland KD, Rosowski JR, Gretz MR, Roemer SC (1993) Diatom extracellular polymeric substances: function, fine structure, chemistry, and physiology. J Phycol 29:537–566

Hofmann T, Hanlon ARM, Taylor JD, Ball AS, Osborn AM, Underwood GJC (2009) Dynamics and compositional changes in extracellular carbohydrates in estuarine sediments during degradation. Mar Ecol Prog Ser 379:45–58

Kocum E, Underwood GJC, Nedwell DB (2002) Simultaneous measurement of phytoplanktonic primary production, nutrient and light availability along a turbid, eutrophic UK east coast estuary (the Colne Estuary). Mar Ecol Prog Ser 231:1–12

Lucas CH, Widdows J, Wall L (2003) Relating spatial and temporal variability in sediment chlorophyll *a* and carbohydrate distribution with erodibility of a tidal flat. Estuaries 26:885–893

Macko SA, Helleur R, Hartley G, Jackman P (1990) Diagenesis of organic matter — a study using stable isotopes of individual carbohydrates. Org Geochem 16:1129–1137

Macko SA, Ryan M, Engel MH (1998) Stable isotopic analysis of individual carbohydrates by gas chromatographic/combustion/isotope ratio mass spectrometry. Chem Geol 152: 205–210

McConville MJ, Wetherbee R, Bacic A (1999) Subcellular location and composition of the wall and secreted extracellular sulphated polysaccharides/proteoglycans of the diatom *Stauroneis amphioxys* Gregory. Protoplasma 206: 188–200

Middelburg JJ, Barranguet C, Boschker HTS, Herman PMJ, Moens T, Heip CHR (2000) The fate of intertidal microphytobenthos carbon: an *in situ* ^{13}C-labeling study. Limnol Oceanogr 45:1224–1234

Moore-Kucera J, Dick RP (2008) Application of ^{13}C-labeled litter and root material for *in situ* decomposition studies using phospholipid fatty acids. Soil Biol Biochem 40: 2485–2493

Paterson DM (1986) The migratory behaviour of diatom assemblages in a laboratory tidal micro-ecosystem examined by low temperature scanning electron microscopy. Diatom Res 1:227–239

Paterson DM (1989) Short-term changes in the erodibility of intertidal cohesive sediments related to the migratory behavior of epipelic diatoms. Limnol Oceanogr 34:223–234

Silfer JA, Engel MH, Macko SA, Jumeau EJ (1991) Stable carbon isotope analysis of amino acid enantiomers by conventional isotope ratio mass spectrometry and combined gas chromatography/isotope ratio mass spectrometry. Anal Chem 63:370–374

Skoog A, Benner R (1997) Aldoses in various size fractions of marine organic matter: implications for carbon cycling. Limnol Oceanogr 42:1803–1813

Smith DJ, Underwood GJC (1998) Exopolymer production by intertidal epipelic diatoms. Limnol Oceanogr 43: 1578–1591

Stal LJ (2003) Microphytobenthos, their extracellular polymeric substances, and the morphogenesis of intertidal sediments. Geomicrobiol J 20:463–478

Taylor IS, Paterson DM, Mehlert A (1999) The quantitative variability and monosaccharide composition of sediment carbohydrates associated with intertidal diatom assemblages. Biogeochemistry 45:303–327

Teece MA, Fogel ML (2007) Stable carbon isotope biogeochemistry of monosaccharides in aquatic organisms and terrestrial plants. Org Geochem 38:458–473

Thornton DCO, Dong LF, Underwood GJC, Nedwell DB (2002) Factors affecting microphytobenthic biomass, species composition and production in the Colne Estuary (UK). Aquat Microb Ecol 27:285–300

Thornton DCO, Dong LF, Underwood GJC, Nedwell DB (2007) Sediment-water inorganic nutrient exchange and nitrogen budgets in the Colne Extuary, UK. Mar Ecol Prog Ser 337:63–77

Underwood GJC, Paterson DM (2003) The importance of extracellular carbohydrate production by marine epipelic diatoms. Adv Bot Res 40:183–240

Underwood GJC, Smith DJ (1998) Predicting epipelic diatom exopolymer concentrations in intertidal sediments from sediment chlorophyll *a*. Microb Ecol 35:116–125

Underwood GJC, Paterson DM, Parkes RJ (1995) The measurement of microbial carbohydrate exopolymers from intertidal sediments. Limnol Oceanogr 40:1243–1253

Underwood GJC, Perkins RG, Consalvey M, Hanlon ARM, Oxborough K, Baker NR, Paterson DM (2005) Patterns in microphytobenthic primary productivity: species-specific variation in migratory rhythms and photosynthetic efficiency in mixed-species biofilms. Limnol Oceanogr 50: 755–767

van Dongen BE, Schouten S, Damsté JSS (2001) Gas chromatography/combustion/isotope-ratio-monitoring mass spectrometric analysis of methylboronic derivatives of monosaccharides: a new method for determining natural ^{13}C abundances of carbohydrates. Rapid Commun Mass Spectrom 15:496–500

van Duyl FC, de Winder B, Kop AJ, Wollenzien U (1999) Tidal coupling between carbohydrate concentrations and bacterial activities in diatom-inhabited intertidal mudflats. Mar Ecol Prog Ser 191:19–32

van Duyl FC, de Winder B, Kop AJ, Wollenzien U (2000) Consequences of diatom mat erosion for carbohydrate concentrations and heterotrophic bacterial activities in intertidal sediments of the Ems-Dollard estuary. Cont Shelf Res 20: 1335–1349

van Oevelen D, Middelburg JJ, Soetaert K, Moodley L (2006a) The fate of bacterial carbon in an intertidal sediment: modeling an *in situ* isotope tracer experiment. Limnol Oceanogr 51:1302–1314

van Oevelen D, Moodley L, Soetaert K, Middelburg JJ (2006b) The trophic significance of bacterial carbon in a marine intertidal sediment: results of an *in situ* stable isotope labeling study. Limnol Oceanogr 51:2349–2359

Vestal JR, White DC (1989) Lipid analysis in microbial ecology. Bioscience 39:535–541

Veuger B, van Oevelen D, Boschker HTS, Middelburg JJ (2006) Fate of peptidoglycan in an intertidal sediment: an *in situ* ^{13}C-labeling study. Limnol Oceanogr 51:1572–1580

Volkman JK, Jeffrey SW, Nichols PD, Rogers GI, Garland CD (1989) Fatty acids and lipid composition of 10 species of microalgae used in mariculture. J Exp Mar Biol Ecol 128: 219–240

Wainman BC, Smith REH, Rai H, Furgal JA (1999) Irradiance and lipid production in natural algal populations. In: Arts MT, Wainman BC (eds) Lipids in freshwater ecosystems. Springer-Verlag, New York, p 45–70

Wang Y, Lu J, Mollet JC, Gretz MR, Hoagland KD (1997) Extracellular matrix assembly in diatoms (Bacillariophyceae) II. 2,6-Dichlorobenzonitrile inhibition of motility and stalk production in the marine diatom *Achnanthes longipes.* Plant Physiol 113:403–409

White DC, Stair JO, Ringelberg DB (1996) Quantitative comparisons of *in situ* microbial biodiversity by signature biomarker analysis. J Ind Microbiol 17:116–123

Wolfstein K, de Brouwer JFC, Stal LJ (2002) Biochemical partitioning of photosynthetically fixed carbon by benthic diatoms during short-term incubations at different irradiances. Mar Ecol Prog Ser 245:21–31

Wustman BA, Gretz MR, Hoagland KD (1997) Extracellular matrix assembly in diatoms (Bacillariophyceae). I. A model of adhesives based on chemical characterization and localization of polysaccharides from the marine diatom *Achnanthes longipes* and other diatoms. Plant Physiol 113:1059–1069

Wustman BA, Lind JL, Wetherbee R, Gretz MR (1998) Extracellular matrix assembly in diatoms (Bacillariphyceae) III. Organization of fucoglucuronogalactans within the adhesive stalks of *Achnanthes longipes.* Plant Physiol 116: 1431–1441

Zar JH (1999) Biostatistical analysis. 4th edn. Prentice Hall, Englewood Cliffs, NJ

Zelles L (1997) Phopholipid fatty acid profiles in selected members of soil microbial communities. Chemosphere 35: 275–294

Zhou JK, Mopper K, Passow U (1998) The role of surface-active carbohydrates in the formation of transparent exopolymer particles by bubble adsorption of seawater. Limnol Oceanogr 43:1860–1871

Ziegler SE, White PM, Wolf DC, Thoma GJ (2005) Tracking the fate and recycling of ^{13}C-labeled glucose in soil. Soil Sci 170:767–778

Editorial responsibility: Rutger de Wit, Montpellier, France

Submitted: November 12, 2007; Accepted: February 6, 2009
Proofs received from author(s): April 20, 2009